ELECTROCHROMIC AND PHOTOVOLTAIC APPLICATIONS OF
BENZOTRIAZOLE BEARING DONOR ACCEPTOR TYPE CONJUGATED
POLYMERS

A THESIS SUBMITTED TO
THE GRADUATE SCHOOL OF NATURAL AND APPLIED SCIENCES
OF
MIDDLE EAST TECHNICAL UNIVERSITY

BY

DERYA BARAN

IN PARTIAL FULFILLMENT OF THE REQUIREMENTS
FOR
THE DEGREE OF MASTER OF SCIENCE
IN
CHEMISTRY

FEBRUARY 2010

Approval of Thesis

ELECTROCHROMIC AND PHOTOVOLTAIC APPLICATIONS OF BENZOTRIAZOLE BEARING DONOR ACCEPTOR TYPE CONJUGATED POLYMERS

submitted by **DERYA BARAN** in partial fulfillment of the requirements for the degree of **Master of Science in Chemistry Department, Middle East Technical University** by,

Prof. Dr. Canan Özgen   _____
Dean, Graduate School of **Natural and Applied Sciences**

Prof. Dr. İlker Özkan   _____
Head of Department, **Chemistry**

Prof. Dr. Levent Toppare   _____
Supervisor, **Chemistry Dept., METU**

Examining Committee Members:

Prof. Dr. Leyla Aras   _____
Chemistry Dept., METU

Prof. Dr. Levent K. Toppare   _____
Chemistry Dept., METU

Prof. Dr. Duygu Kısakürek   _____
Chemistry Dept., METU

Assoc. Prof. Dr. Serap Güneş   _____
Physics Dept., Yıldız Technical University

Asst. Prof. Dr. Ali Çırpan   _____
Chemistry Dept., METU

                                        Date: 05/02/2010

I hereby declare that all information in this document has been obtained and presented in accordance with academic rules and ethical conduct. I also declare that, as required by these rules and conduct, I have fully cited and referenced all material and results that are not original to this work.

Name, Last Name : Derya Baran

Signature :

ABSTRACT

ELECTROCHROMIC AND PHOTOVOLTAIC APPLICATIONS OF
BENZOTRIAZOLE BEARING DONOR ACCEPTOR TYPE CONJUGATED
POLYMERS

Baran, Derya

M.Sc., Department of Chemistry

Supervisor: Prof. Dr. Levent Toppare

February 2010, 87 pages

Organic semi-conductors are of great interest since these compounds can be utilized as active layers in many device applications such as ECDs, LEDs and solar cells. Incorporating the benzotriazole units into the polymer backbone enhances the optical properties of donor units. Hexyl thiophene and pyrrole are commonly used as electron donor materials. Benzotriazole can be coupled to hexyl thiophene or pyrrole to yield materials which can be polymerized to give donor acceptor type polymers. These materials are promising components in fast switching polymeric electrochromic devices and highly efficient photovoltaic devices. During thesis studies,poly(2-dodecyl-4,7-bis(4-hexylthiophen-2-yl)-2H-benzo[d][1,2,3]triazole) (PHTBT) and poly(2-dodecyl-4,7-di(1H-pyrrol-2-yl)-2H- benzo [d] [1,2,3] triazole) (PPyBT) will be synthesized via N-alkylation, bromination, stannylation and Stille coupling reactions.

Electrochromic and photovoltaic properties of the polymers will be investigated in detail.

Keywords: Electrochromism, Donor-Acceptor Theory, Solar Cells, Fast switching.

ÖZ

BENZOTRİAZOL İÇEREN DONÖR AKSEPTÖR TİPİ POLİMERLERİN ELEKTROKROMİK VE FOTOVOLTAİK UYGULAMALARI

Baran, Derya

Yüksek Lisans, Kimya Bölümü

Tez Yöneticisi: Prof. Dr. Levent Toppare

Şubat 2010, 87 sayfa

Organik yarı iletkenler; elektrokromik cihazlar, ışık yayan diyotlar ve güneş pillerinde aktif katman olarak kullanılabildikleri için ilgi çekmektedirler. Donör-Akseptör teoriye göre sentezlenmiş benzotriazol içeren polimerler organik elektronik cihazlar için uygun adaylar olmuşlardır. Polimer zincirine benzotriazol birimleri eklemek bu malzemelerin optik özelliklerini artırmıştır. Benzotriazol hekzil tiyofen ya da pirole katılarak polimerleştirilip donör-akseptör tipi polimerler olarak kullanılabilirler. Bu malzemeler hızlı dönüşümlü elektrokromik cihazlarda ve yüksek verimli güneş pillerinde kullanıılabilecek güçlü adaylardır.Tez çalışmaları boyunca,poli(2-dodesil-4,7-bis(4-hekzilthiyofen-2-il)-2H-benzo[d][1,2,3]triazol) (PHTBT) ve poli(2-dodesil-4,7-di(1H-pirol-2-il)- 2H-benzo [d] [1,2,3] triazol) (PPyBT) N-alkilasyon, bromlama, kalaylama ve Stil birleştirme reaksiyonlarıyla sentezlenip polimerleştirilecek ve bu polimerlerin elektrokromik ve fotovoltayik özellikleri detaylı olarak çalışılacaktır.

Anahtar Sözcükler: Elektrokromizm, donör-akseptör polimerler, güneş pilleri, hızlı renk geçişi

To My Family

ACKNOWLEDGMENTS

TABLE OF CONTENTS

LIST OF FIGURES

xviii

LIST OF TABLES

CHAPTER 1

INTRODUCTION

1.1   Conducting Polymers

As we enter the era of intelligent materials and embark upon a new approach to material design and synthesis, certain groups of materials are emerged as champions. Even the most cursory glance at the components used by nature in the development of material systems and structures reveals that polymers are extremely powerful in this regard.

It was a breakthrough when Alan Heeger, Hideki Shirakawa and Alan MacDiarmid were awarded with the Nobel Prize in chemistry (2000) for showing how plastic can be made to conduct electric current. The discovery that polyacetylene (PA) can be made to conduct electricity upon doping, opened a new field for conducting polymers.[1-3] The finding of this class of materials was very promising as they exhibit a unique combination of properties of metals and plastics such as electrical conductivity, optical activity, flexibility and processability.[4-7]

Mankind's ability to design polymers from the molecular level, coupled with a better understanding of structure-property relationships enabled the design of more sophisticated conducting polymers like polythiophenes, polypyrroles and many others having better properties than PA. [8-14] (Figure 1.1)
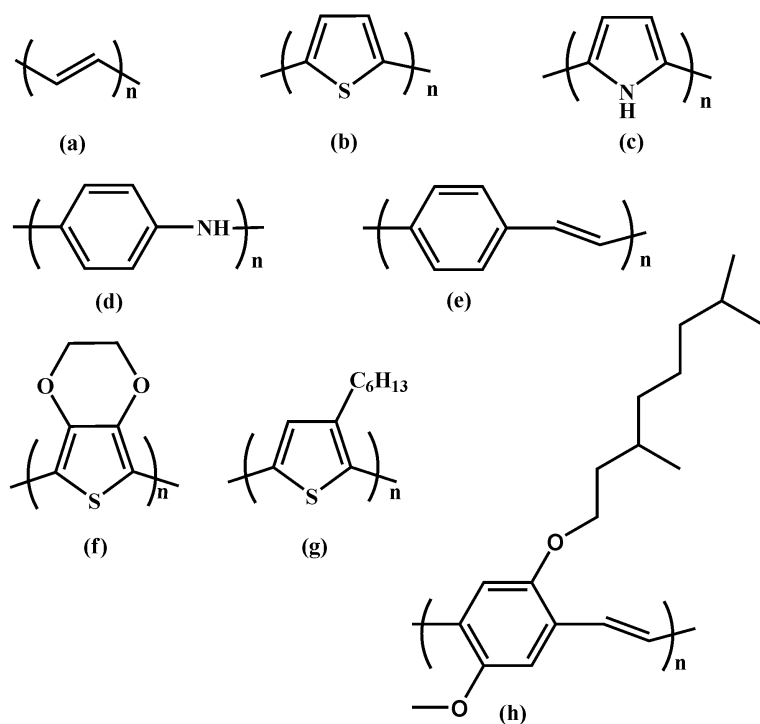
Figure 1. 1 Chemical structures of some common conjugated polymers: (a) Polyacetylene, (b) polythiophene, (c) polypyrrole, (d) polyaniline, (e) poly(p-phenylenevinylene), (f) poly(3,4-ethylenedioxy-thiophene), (g) poly(3-hexylthiophene), (h) (poly-[2-(3,7-dimethyloctyloxy)-5-methyloxy]-para-phenylene-vinylene)(MDMO-PPV)

1.2 Conjugated Polymers

The known fact that available plastics are insulators stem from the formation of σ bonds between the constituent carbon atoms. Yet, in conjugated polymers (Figure 1.1), e.g., polyacetylene, the situation is different: In these polymers, the bonds between the carbon atoms that form the backbone are

2

alternatingly single or double (see Figure 1.2); this property is called *conjugation*. In the backbone of a conjugated polymer, each carbon atom binds to only three adjacent atoms, leaving one electron per carbon atom in a p_z orbital. The mutual overlap between these p_z orbitals results in the formation of π bonds along the conjugated backbone, thereby delocalizing the π electrons along the entire conjugation path. The delocalized π electrons fill up to whole band and, therefore, conjugated polymers are intrinsic semiconductors. The filled π band is called the highest occupied molecular orbital (HOMO) and the empty π^* band is called the lowest unoccupied molecular orbital (LUMO). The energy difference between HOMO and LUMO levels defines the band gap of the polymer. Optical measurements revealed that band gap of most known conjugated polymers ranges from 1 to 4 eV. [15] This π system can be excited without the chain, held together by the σ bonds, falling apart. Thus, it is possible to promote an electron from the HOMO to the LUMO level upon, for example, light absorption.
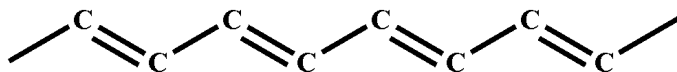
Figure 1. 2 In polyacetylene, the bonds between adjacent carbon atoms are alternatingly single or double.

1.3   The Concept of Doping Applied to Conjugated Polymers

The report of Shirakawa et al. [1-3] showed that the electrical conductivity of polyacetylene can be increased by several orders of magnitude through reaction with an oxidative agent or electron acceptor (p-doping) or a reducing agent or electron donor (n-doping). Doping is the process of intentionally introducing or removing impurities into/from an extremely pure (also referred to as *intrinsic*)

3

semiconductor to change its structural and electrical properties. This process can be accomplished by chemical, photochemical or electrochemical means.[4] The conjugated polymers contain electronic states that can be reversibly emptied or filled with electrochemical techniques resulting in metal-insulator transitions which have potential for practical applications. [16-22]

In conjugated polymers, small amount of dopant gives rise to large changes of the properties of the material. Doping can be done chemically using reducing or oxidizing agents or electrochemically by applying a certain voltage in a suitable medium. The basic processes are shown in reactions (1) and (2) as examples for chemical and electrochemical doping, respectively.

p-doping $\quad (\pi\text{-polymer}) + A \rightarrow (\pi\text{-polymer})^+ A^-$ (1)

$(\pi\text{-polymer}) + [Li^+(ClO_4^-)]_{solv} \rightarrow [(\pi\text{-polymer})^{x+}(ClO_4^-)_x] + xLi^+ + xe^-$ (2)
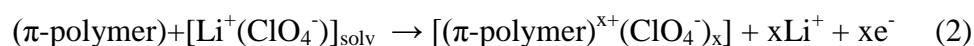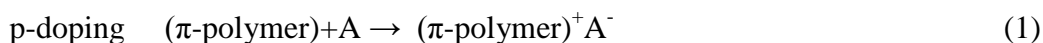
As seen in both cases, compensation of the generated charge is needed. Similarly, n-doping results in partial reduction of the polymer chain, as shown in reactions (3) for chemical doping and (4) for electrochemical doping.

n-doping $\quad (\pi\text{-polymer}) + D \rightarrow (\pi\text{-polymer})^- D^+$ (3)

$(\pi\text{-polymer}) + xe^- + [Li^+(ClO_4^-)]_{solv} \rightarrow [(\pi\text{-polymer})^{x-}(Li^+)_x] + x(ClO_4^-)$ (4)
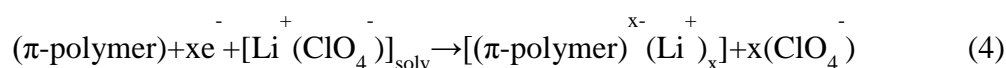
Chemical and electrochemical doping generally gives similar results by means of the properties of the induced charges. The main advantage of electrochemical doping over the chemical way lies in the control of the doping level. This can easily be done electrochemically via the applied voltage giving highly reproducible results, whereas with chemical doping attempts to reach

intermediate doping levels often result in inhomogeneous doping. The p-doping process has been investigated in a greater extent than n-doping due to the need of dry and oxygen-free environments.[23] Therefore, there are handful studies exploring n-dopable materials since negatively charged polymer chains can easily be oxidized due to the oxidizing agents in air.[24]

1.4 Charge Carriers in Conjugated Polymers: Solitons, Polarons and Bipolarons

Solitons

Trans-polyacetylene is a polymer with a degenerate ground state since the double and single bonds can be interchanged without changing the ground state energy. Therefore the ground state has two configurations A and B with the same energy as shown in Figure 1.3.
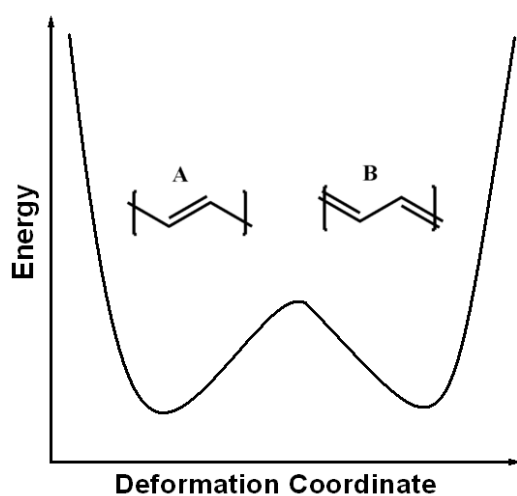
Figure 1. 3 Potential energy curve for trans-polyacetylene showing the two equivalent structures

If both of the energetically equivalent configurations coexist on the same chain, a structural defect will occur at their interface. This defect is called a (neutral) soliton, which consists of a single unpaired electron that can extend over approximately ten carbon atoms [25].

Doping adds or removes an electron to or from this state during n- or p-doping leading to a negatively or positively charged soliton, which can also be called spinless anion or cation. A band diagram for neutral, positive and negative soliton is shown in Figure 1.4. Associated with these three types of solitons new optical transitions depending on their symmetry allowance can be observed in optical absorption spectra, which are indicated with dotted arrows in Figure 1.4.
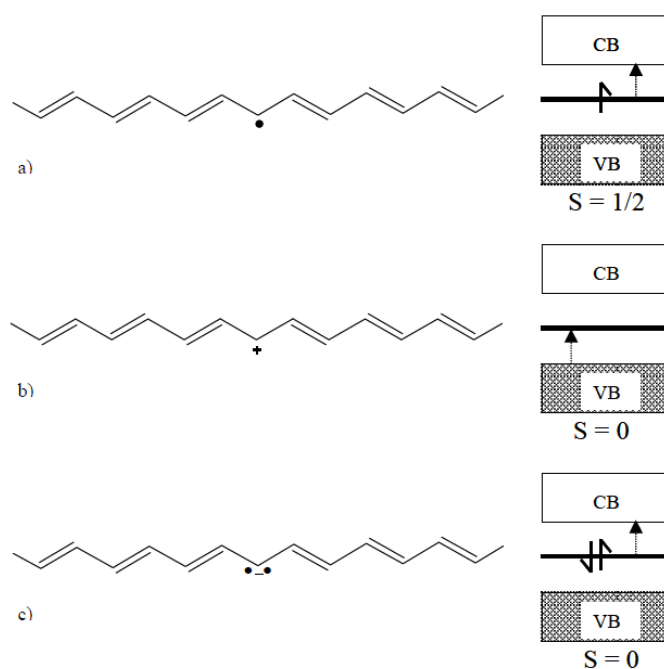
Figure 1. 4 Soliton structures in polyacetylene and corresponding electronic states in the band gap, a) neutral soliton, b) positive soliton, c) negative soliton; only the neutral soliton carries a spin (S)

Polarons and Bipolarons

Most other conjugated polymers have two energetically inequivalent bond alternation structures, which means they have a non-degenerate ground state.[26] For example in poly(p-phenylenevinylene) (structure is shown in Figure 1.5) the quinoid structure (B) is less stabilized and therefore higher in energy than the benzenoid form (A). Figure 1.5 shows the energy diagram for these two structures.
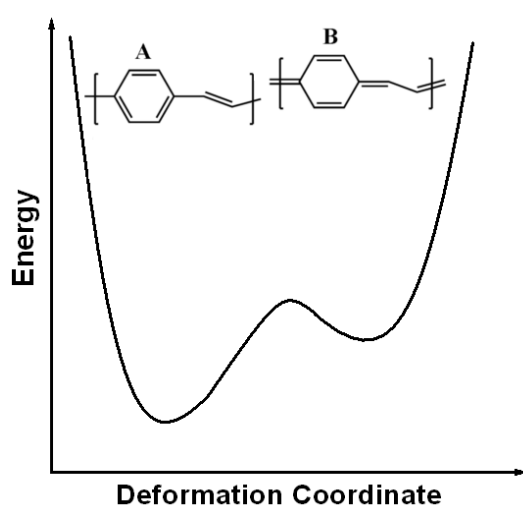
Figure 1. 5 Potential energy curve for poly(p-phenylenevinylene) with its energetically inequivalent structures, benzenoid (A) and quinoid (B).

Upon p- or n-doping charge carriers called polarons (radical cation or anion) and bipolarons (spinless dication or dianion) are formed and two new electronic states are created in the π-π^* band gap. A band scheme of the above described is given in Figure 1.6. The dotted arrows indicate new possible optical transitions. [27]
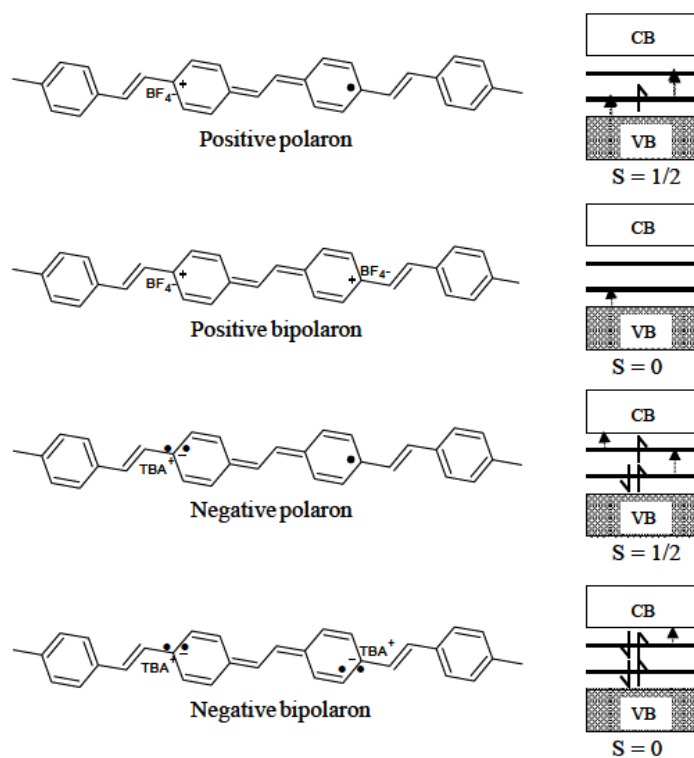
Figure 1. 6 Polaron and bipolaron structures in poly(p-phenylenevinylene) with their corresponding electronic states in the band gap; only positive and negative polaron carry a spin (S),bipolarons are spinless.

1.5 Applicatons of Conjugated Polymers

Conjugated polymers have been used in few large-scale applications up to 21st century due to their poor processability. However, they attracted attention rapidly in new applications with increasingly processable materials with better electrical and physical properties and lower costs. New structural designs of conjugated polymers provided fresh air to a lot of field including: Organic Light

Emitting Diodes (OLEDs) [28], Organic Field Effect Transistors (OFETs) [29] ,Organic Solar Cells (OSCs) [30] and Electrochromic Devices (ECDs) [31]. Polymers that are applicable to many fields are regarded as multi-purpose materials. These conjugated polymers are unique since they offer great potential to be used in LEDs, OSCs and ECDs.

1.5.1   Light Emitting Diodes

A Light Emitting Diode (LED) is a semiconductor light source. LEDs present many advantages over incandescent light sources including lower energy consumption, longer lifetime, improved robustness, smaller size, faster switching, and greater durability and reliance.[32] If the emitting layer material of the LED is an organic compound, it is known as an Organic Light Emitting Diode (OLED). To function as a semiconductor, the organic emitting material must have conjugated π-bonds. The emitting material can be a small organic molecule in a crystalline phase, or a conjugated polymer. Polymeric materials can be flexible. Compared with regular LEDs, OLEDs are lighter, and polymer LEDs can have the added advantage of being flexible.

1.5.2   Organic Field Effect Transistors

An Organic Field-Effect Transistor (OFET) is a field effect transistor using an organic semiconductor in its channel. OFETs can be prepared either by vacuum evaporation of small molecules, or simply by solution-casting of polymers or small molecules. Common feature of OFET materials is the inclusion of an aromatic or otherwise conjugated π-electron system, facilitating

the delocalization of orbital wavefunctions. [33] Electron withdrawing groups or donating groups can be attached that facilitate hole or electron transport.

OFETs employing many aromatic and *conjugated materials* as the active semiconducting layer have been reported, including polymers such as polythiophenes (especially poly3-hexylthiophene (P3HT), polyfluorene, polydiacetylene, poly 2,5-thienylene vinylene, poly p-phenylenevinylene (PPV). [34]

1.5.3   Organic Solar Cells

Organic materials gained unforeseen rapid interest for implementing them in photovoltaic solar cells in the past decade. [35] Since the report of first thin film solar cell by Tang, [36] many concepts have been presented using small molecules, combinations of organic inorganic materials and conjugated polymers. [37] A solar cell is a device that converts sunlight into electricity. Conjugated polymers are of high interest as the third generation solar cells due to several reasons including; processability and flexibility. [38] Low bang gap materials offer great potential to be used as active layers in organic solar cells since their lower energy transitions fit into the solar spectrum and lead to a better match (Figure 1.7). [39]
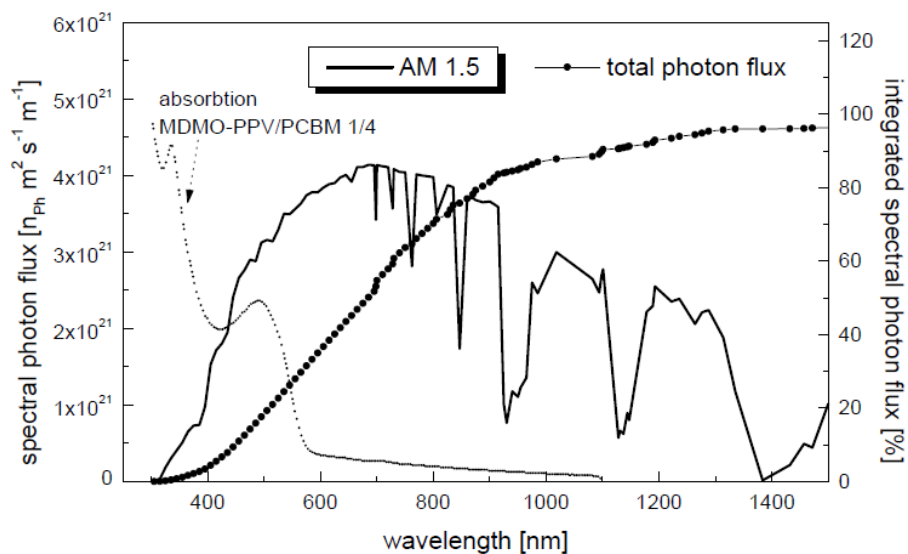
Figure 1. 7 The terrestrial AM1.5 sun spectrum (..) and the integrated spectral photon flux (starting from 0 nm) (-.-) in comparison with the absorption of the active layer (---) of an MDMO-PPV/PCBM solar cell.

1.5.3.1 Advantages of Organic Semiconductors

Organic semiconductors, including conjugated polymers, are promising materials for solar cells since they are cheap in production and production and purification can be done at room temperature. Furthermore, organic chemistry can tailor the materials according to the demand. Organic devices based on conjugated polymers are flexible, lightweight and easy to produce [38]. Polymer processing done by spin casting, doctor blading [40] has been successfully applied for solar cells preparation, ink-jet printing or of even roll-to-roll processing are well known techniques and could be principally used for device fabrication.

11

1.5.3.2 Concept of Bulk Heterojucntion Solar Cells

Bilayer devices, consisting of a p and n type organic semiconductor (donor and acceptor, respectively) were the forerunners in organic solar cells until the invention of bulk heterojunction (BHJ). Due to the limited charge generation between donor/acceptor interface and the short lifetime of the charged species, the conversion efficiencies of such devices were restricted. [41] With the bulk heterojunction architecture, an efficient charge generation in the whole active layer is ensured by blending the conjugated polymer (donor) and C_{60} or soluble derivatives of fullerenes (acceptor) (Figure 1.8). [42] Very soon, power efficiencies of 1 % were reached. Intensive studies and engineering skills pushed up the efficiencies up to considerable values.

(a)   (b)
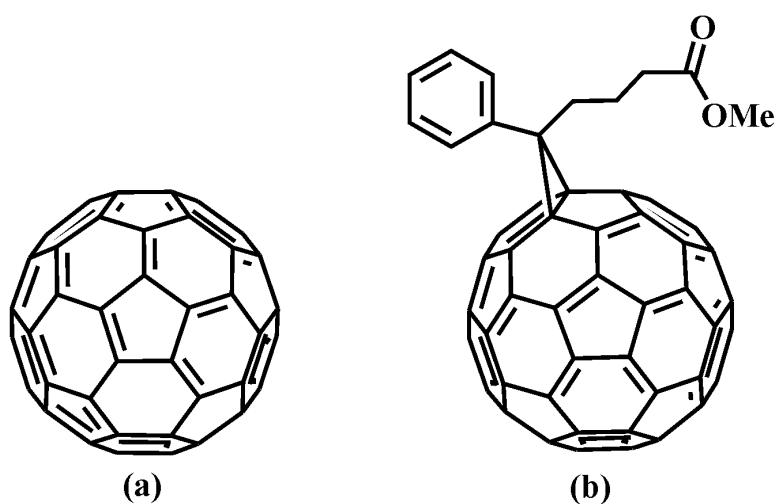
Figure 1. 8 Structure of C_{60} (a) its soluble form [6,6]-phenyl-C_{61}-butyric acid methyl ester (PCBM) (b).

12

1.5.3.2.1 Principles of Bulk Heterojunction Solar Cells

In order to get electricity from sun light, three steps are to be fulfilled by solar cells;

- Absorption of light
- Generation of charge carriers
- Transportation of opposite charges to opposite contacts.

The general procedure to obtain electricity is the same for all solar cells, but polymer-fullerene solar cells are described in this thesis.

The HOMO-LUMO (π-π^*) excitation from the valence band to the conduction band in a conjugated polymer can be achieved with a light energy higher than the band gap of the material. These excited electrons can be converted into current. Therefore, the amount of absorbed light is directly related to current. Absorption spectrum of the material and the thickness are two main parameters. Absorption spectrum should match with solar spectrum and thickness cannot exceed a certain limit because of the limited mobility of charge carriers.The most efficient way for charge generation is the photoinduced charge transfer from polymer to fullerene (Figure 1.9). [43] When light comes, absorption of photons result in the formation of excitons (strongly bounded electron-hole pair).

In the third step, the created charges are seperated and transported selectively to the contacts. The holes are transported by the polymer to ITO contact and the electrons to the metal contact (Al). When charges are collected in the contacts, electricity is produced.
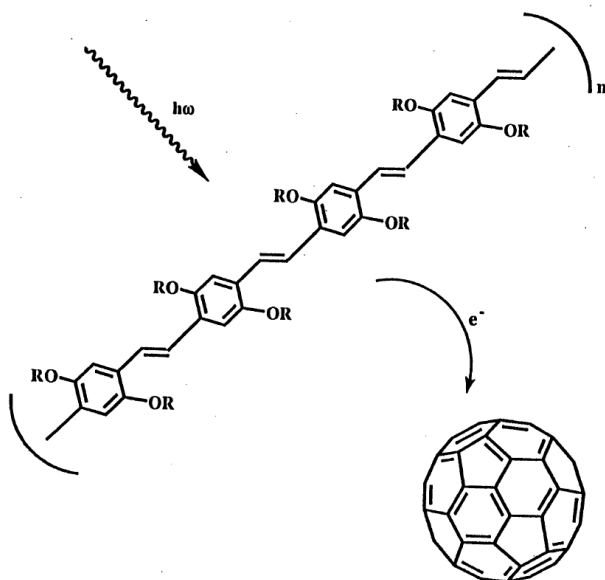
Figure 1. 9 Photoinduced charge transfer from photoexcited PPV to C$_{60}$.

1.5.3.3 Device Fabrication and Characterization

      A BHJ solar cell has a typical structure shown in Figure 1.10. The polymer/ PCBM blend is sandwiched between two electrodes serving as the anode and cathode. The glass substrate is coated with Indium Tin Oxide (ITO) which is a transparent electrode with a high work function, suitable as the anode. To reduce the roughness of the ITO layer and to act as a hole injection layer, a poly (3-4 ethylenedioxythiophene) (PEDOT): poly(styrenesulfonate) layer (5.1 eV) is spin cast, followed by the active layer (polymer: PCBM blend). The top electrode is usually a low work function metal such as Aluminum (Al), Lithium fluoride (LiF) or Calcium (Ca).
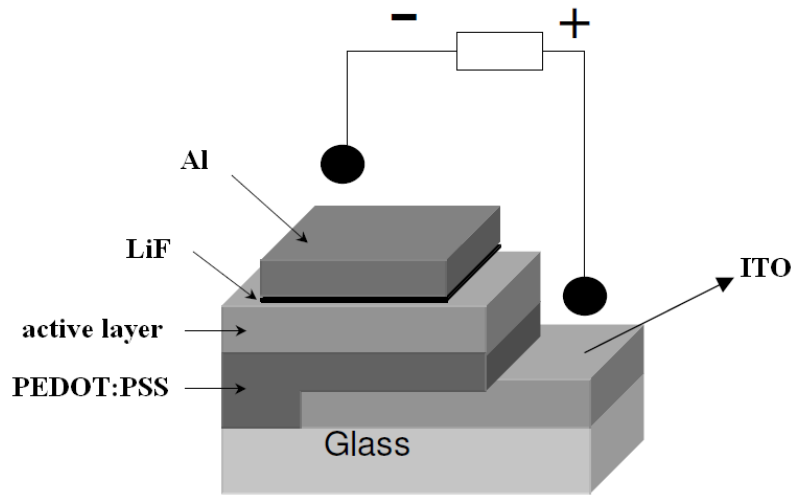
Figure 1. 10 Device architecture of a Bulk Heterojunction Solar Cell

To study the performance of the photovoltaic devices, current-voltage (*I-V*) measurements are done under dark and illumination. A typical current-voltage charateristic of a solar cell under illumination can be seen in Figure 1.11. The current density under illumination at zero applied potential is called the short-circuit current density *Jsc*. The maximum voltage that the cell can supply, where the current-density is zero is stated as open-circuit voltage *Voc*. The fill factor FF is defined as the maximum power that can be gathered from the device to open-circuit voltage and short-circuit current. The power conversion efficiency ($\eta\%$) is related to these variables by equation :

$$\eta \ \% = (Jsc \ \times \ Voc \ \times \ FF) \ / \ I \qquad (5)$$

where I is the light intensity. The efficiencies should be measured under standard test conditions. The conditions include the temperature of the cell (25°C), the light intensity (1000 W/m2) and the spectral distribution of light (AM 1.5).
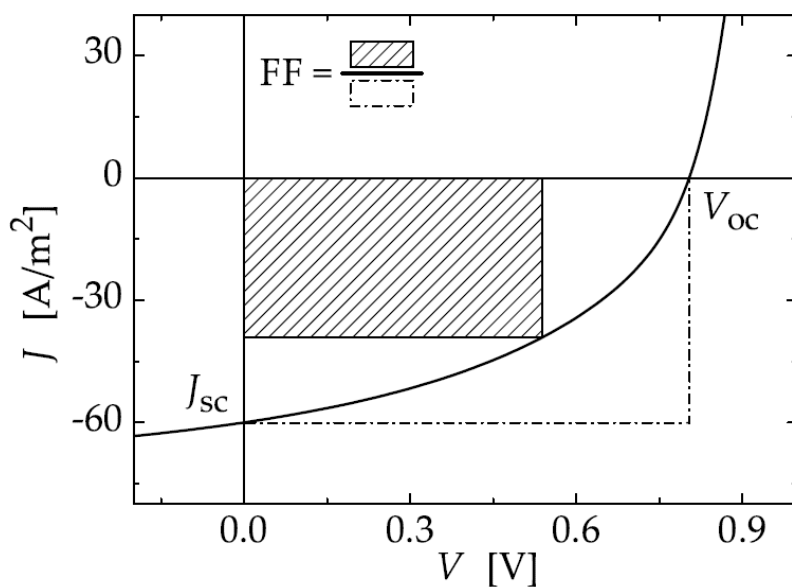
Figure 1. 11 Typical current-voltage characteristic of a Bulk Heterojunction solar cell

1.5.4 Electrochromic Devices

Electrochromic Devices (ECDs) using electrochemically active conjugated polymers have been widely investigated. [44] Conjugated polyheterocycles such as polyanilines, polypyrroles, polythiophenes and exclusively poly(3-4 ethylenedioxythiophene) (PEDOT) and its derivatives have been reported as

electrochromic materials. [45] These materials provide color changes within the visible spectrum between two colored states or a transmissive state when either p- or n-doped. Low band gap conjugated polymers possess a variety of intrinsic properties such as highly transmissive oxidized states, stability in electrochemical p- and n- doping and extended absorption spectrum ranges to near-IR region. [46] Based on these properties, such polymers are concieved as unique elechrochromic materials. Foreseen great attention is given to these polymers since they have potential to be applicable to infrared ECDs.

1.5.4.1 Electrochromism

Electrochromism is defined as the reversible, persistent and visible change in color or more precisely in optical properties of a material upon applied electric field (p- or n- doping). During doping, structural modifications on the polymer backbone is accompanied by a change in the electronic transitions from a higher energy to lower energy. Since these transitions lie in the visible region, most of the electrochromic materials change their colors between two colored states. When the lower transitions go further to near-IR region, the material reveals a transmissive state and a colored state or vice versa. These properties of the conjugated polymers are highly dependent on band gap. The crucial properties of electrochromic materials other than band gap are their switching times, contrast ratios between oxidized and reduced states and coloration efficiencies which determine the injected/ejected charge per unit area.

1.5.4.2 Advances in Electrochromism

In recent years, many intelligent materials are designed and synthesized to serve as electrochromic materials. Extensive studies are performed in order to characterize such materials to obtain high contrast ratio,fast switching time, stable oxidized states and fine color tuning. Polyaniline was the pioneer when first reported by Goppelsröder in 1876 [47] where conjugated polymers started to be used as active layer in elechrochromic materials. Oxidative polymerization of aniline (colorless) in solution yields polyaniline which changes its color upon reduction and oxidation.

The electrochromism of polypyrrole was first studied by Diaz et al 1979. [48] Reduction of the polypyrrole film results in pale-yellow and in oxidation polymer film exhibits dark-blue color.Thiophene and its derivatives took great interest in variation of color. There has been many studies based on thiophene and thiophene based structures including oligomers. After the discovery of Donor-Acceptor (D-A) approach to decrease the bang gap and alter the properties of polymers, many reports have been published on these conjugated polymers. [45] Achieving solubility in these polymers made them inevitable candidates to be used for multi-purposes. [49] Even multi-color materials (including black and transmissive states) are now can be easily achieved using D-A type monomer structures. [50] Beyond these studies, these invaluable designs of monomers should be used for other fields including solar cells and light emitting diodes since they are processable, flexible and low cost materials.

1.6   Polymerization Methods

There are several numbers of methods to synthesize conducting polymers namely chemical polymerization, electrochemical polymerization, photochemical polymerization, concentrated emulsion polymerization, solid-state polymerization and soluble precursor polymer preparation. Conducting polymers that are stable in both conducting and undoped states and soluble in certain solvents were synthesized in order to obtain new and novel structures, where the order of the polymer backbone as well as conductivity was increased.

1.6.1   Chemical Polymerization

In chemical polymerization which is the least expensive, most simple, and most widely used chemical synthesis of conducting polymers [51], stoichiometric amount of oxidizing reagent is used to produce polymer in its doped or conducting form. Heterocyclic monomers are usually polymerized with $FeCl_3$ as the chemical oxidant although other oxidants can also be employed. [52] Reduction to the neutral state is accomplished by the addition of a strong base such as ammonium hydroxide or hydrazine.

Chemical polymerization occurs in the bulk of the solution, and the resulting polymers precipitate as insoluble solids having limiting degree of polymerization. Overoxidation and decomposition may also occur in such polymerization if strong oxidizing agents are used. [53]

1.6.2 Electrochemical Polymerization

Electropolymerization is achieved by the electro-oxidation of the monomer in an inert organic solvent containing supporting electrolyte. Electrochemical syntheses of poly(heterocycles) have been carried out by an anodic or a cathodic route. Electrochemical synthesis is a simple, selective and reproducible method where the type of solvent, electrolyte system, choice and concentration of monomer and electrodes strongly affect the properties of the final conducting polymer. Compared with other chemical and electrochemical methods, the advantages of oxidative electropolymerization are [54]:

(i) A highly electrochemically active and conductive polymer film can be easily produced on an electrode, which can be directly used as an electrode in a battery or a sensor.

(ii) Film thickness, morphology and conductivity can be easily controlled by the applied potential, polymerization time, and the electrochemical potential scan rate.

(iii) They provide an in situ way to investigate the polymerization process and the properties of the resulting conducting polymer by electrochemical or spectroscopic techniques.

1.7   Poly(3-alkylthiophene)s

Although poly(*p*-phenylene vinylene) (PPV) derivatives were the touchstone in solar cells, introducing poly(3-alkyl thiophenes) (P3AT) to BHJ system triggered a broad research in this area. [55] In the history of organic photovoltaics, P3ATs have been of high interest due to their good solubility, processability and environmental stability. [56] The red shifted absorption of a P3AT derivative, poly(3-hexylthiophene) (P3HT), compared to PPVs such as poly[2-methoxy-5-(3',7'-dimethyloctyloxy)-1,4-phenylene vinylene) (MDMO-PPV) resulted in a two fold increase in photocurrent. [57] Hence, photovoltaic devices with 1.5 % power conversion efficiencies were obtained. [58] After the realization of these materials' promising potential for highly efficient solar cells, many studies were focused on PATs. Annealing of P3HT/PCBM active layer in organic solar cells was found to enhance the efficiency [59] with the increased degree of crystallinity. [60]

Postproduction treatments such as applying external voltage or thermal treatment led to an overall increase in conversion efficiencies of devices since the free volume and defect density at the interfaces are reduced. [61] The influence of the work function of materials was also studied in organic solar cells to enhance the V_{oc} and thus the efficiency. [62]

As a further step for the development of plastic solar cells, regioregular poly(3-alkylthiophenes) such as poly(3-hexylthiophene) (P3HT), poly(3-octylthiophene) (P3OT) and poly(3-dodecylthiophene) P3DDT were used as electron donors in polymer:fullerene bulk heterojunction solar cells. [63] Moreover, use of chlorobenzene instead of chloroform and toluene as the solvent increased the efficiencies up to 5.1 %. [64] BHJ solar cell performances have been gradually improved, power conversion efficiencies (PCE) of 5-6 % have been reported and different approaches to improve the efficiency of P3HT/PCBM cells are still being reported. However, the relatively small energy difference between

the HOMO of P3HT and the LUMO of the fullerene acceptor results in a low open-circuit voltage, V_{oc} = 0.6 V [65] which limits the efficiency. This necessitates finding new candidates for further improvements in the field. [66]

1.8   Polypyrroles

Since its first use in electrochemical devices by Diaz et.al [9] polypyrrole was employed in many electronic applications due to the ease of polymerization both chemically and electrochemically. Thin films of the parent polypyrrole are yellow/green (Eg =2.7 eV) in the undoped insulating state and blue/violet in the doped conductive state. [47] Pyrrole was recently used as the donor group with quinoxaline derivatives to give green to transmissive electrochromic polymers. To notice, green to transmissive polymers are very rare since to achieve green color it requires two absorption maxima in visible region which should respond the applied potential simultaneously. Insertion of pyrrole into the DA type polymers with new acceptor units are significantly important since they can combine the ability of both p and n doping with the property of transparency of low band gap systems synthesized from easily oxidized monomers.

1.9   Motivation

Polymers that are applicable to many fields are regarded as multi-purpose materials offering great potential to lower the cost of active layer production for organic electronics. The attractive properties of CPs are mostly based on the ability to alter the electronic and spectral properties with chemical structural modifications. Tailoring the band gap (Eg) of CPs allows variation in emission wavelength, absorption in the visible region and the type of charge carriers upon doping.

22

From the synthetic point of view, the Donor- Acceptor-Donor (D-A-D) route is the most utilized method in terms of diversity in synthetic possibilities while avoiding the solubility limits. Therefore, in this thesis two D-A-D type monomers containing benzotriazole as the acceptor and pyrrole and hexylthiophene as the donor units were synthesized; PyBT and HTBT ((2 dodecyl-4,7-di(1H-pyrrol-2-yl)- 2H- benzo [d] [1,2,3] triazole) and (2-dodecyl-4,7-bis(4 hexylthiophen-2-yl)-2H-benzo[d][1,2,3]triazole), respectively). The chemical polymers of the designed structures in this thesis are used as the donor and the soluble fullerene derivative, [6,6]-phenyl-C_{61}-butyric acid methyl ester (PCBM), is used as the acceptor. Polymers were investigated in detail within both electrochemical and photovoltaic concepts as multifunctional materials. Two polymers were soluble in common organic solvents and revealed outstanding properties. Various properties of the polymers showed that these materials can also be used in OLEDs and OFETs.

CHAPTER 2

EXPERIMENTAL

2.1   Materials

Iron (III) chloride (Aldrich), NaOH (Merck), tetrabutylammonium hexafluoro phosphate ($TBAPF_6$) (Aldrich), PEDOT: PSS (Baytron) were used as received. Thiophene (Aldrich) was distilled before use. Dichloromethane (DCM) (Merck), Chlorobenzene (CB) (Aldrich), nitromethane (Aldrich), methanol (Merck), tributyl tin chloride (Aldrich), N-butyl lithium (Aldrich) and 3-hexylthiophene) (Aldrich) were used without further purification. Anhydrous acetonitrile (ACN) and tetrahydrofuran (THF) purchased from Acros were used as received.

2.2   Equipments

The cyclic voltammograms were recorded using VoltaLab PST050 and Solartron 1285 potentiostats. Measurements were performed at room temperature. A VoltaLab PST050 and a Solartron 1285 Potentiostats were used to provide a constant potential in the electrochemical polymerization. These devices can maintain the voltage difference between the working and reference electrodes at a constant desired value during the electrolysis and compensate for the voltage drop in the electrolysis solution. Electrolyses were performed in a one-compartment cell which was open to air atmosphere unless otherwise mentioned. The working electrode was ITO, counter electrode was platinum (Pt) and the reference

electrode was Ag/AgCl quasi reference electrode (QRE). After each measurement the QRE was calibrated with ferrocene. The potential of QRE was determined as 50 mV versus the normal hydrogen electrode (NHE). All the data reported in this work are measured against this reference electrode.

A Varian Cary 5000 UV-Vis spectrophotometer was used to perform the spectroelectrochemical studies of polymer. Colorimetry measurements were done via a Conica Minolta CS-100 spectrophotometer. ^{1}H-NMR and ^{13}C-NMR spectra of the monomers and the catalytically produced polymer were recorded on a Bruker-Instrument-NMR Spectrometer (DPX-400) with $CDCl_3$ as the solvent and chemical shifts (δ) were given in ppm relative to tetramethylsilane as the internal standard. Fluorescence measurements were conducted using a Varian Eclipse spectrofluorometer. Column chromatography of products was performed using Merck Silica Gel 60 (particle size: 0.040–0.063 mm, 230–400 mesh ASTM). Reactions were monitored by thin layer chromatography with fluorescent coated aluminum sheets. Solvents used for spectroscopy experiments were spectrophotometric grade. All current–voltage (I–V) characteristics of the photovoltaic devices were measured using a Keithley SMU 236 under nitrogen in a dry glove box. A Steuernagel solar simulator for AM 1.5 conditions was used as the excitation source with an input power of 100 mW/cm^2 white-light illumination, which was calibrated using a standard crystalline silicon diode. The solar cells were illuminated through the ITO side. The spectrally resolved photocurrent (IPCE) was measured with an EG&G Instruments 7260 lock-in amplifier. The samples were illuminated with monochromatic light of a Xenon lamp.

2.3   Procedure

2.3.1   Synthesis

2.3.1.1 2-Dodecylbenzotriazole
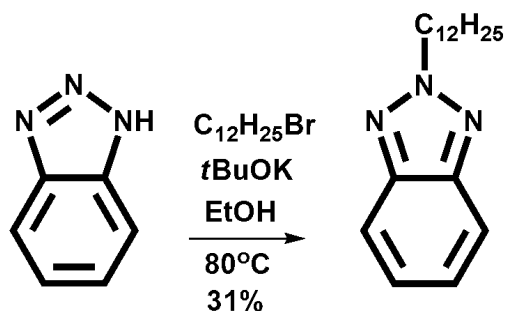
Figure 2. 1 Synthetic route for 2-dodecylbenzotriazole

Synthesis of 2-dodecylbenzotriazole was performed according to methodology described in the literature for a similar compound. 1,2,3-Benzotriazole (5.0 g, 42 mmol), potassium tert-butoxide (5.0 g, 44 mmol), and bromododecane (12.2 g, 49 mmol) were dissolved in methanol (50 mL). The mixture was refluxed for 12 h and monitored by TLC. After removal of the solvent by evaporation, the residue was dissolved in $CHCl_3$ and extracted with water. The organic extract was dried over $MgSO_4$ and the solvent was evaporated under reduced pressure. The residue was subjected to column chromatography (3:2 chloroform:hexane; Rf, 0.29) to obtain 2-dodecylbenzotriazole as a colorless oil (3.7 g, 31%).

2.3.1.2 4,7-Dibromo-2-dodecylbenzotriazole
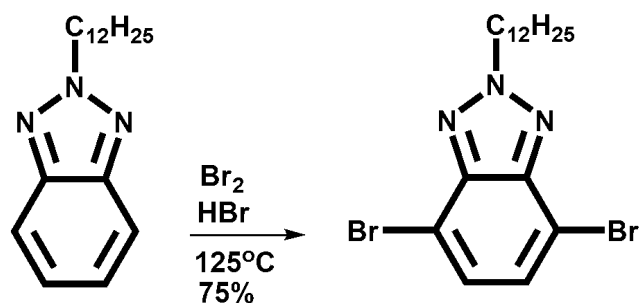
Figure 2. 2 Synthetic route for 4,7-dibromo-2-dodecylbenzotriazole.

2-Dodecylbenzotriazole (3.7 g, 13.1mmol) and an aqueous HBr solution (5.8 M, 15 mL) were added to a flask, and the mixture was stirred for 1 h at 100 °C. Bromine (5.9 g, 36 mmol) was added and the mixture was stirred for 12 h at 135 °C. After the mixture was cooled to room temperature, an aqueous solution of $NaHCO_3$ was added and the product was extracted with $CHCl_3$. The organic layer was dried over $MgSO_4$ and the solvent was evaporated under reduced pressure. With column chromatography (1:1 chloroform:hexane; Rf, 0.33), 4,7- dibromo-2-dodecylbenzotriazole was obtained as light yellow oil (4.3 g, 75%).

2.3.1.3 N-tert-Butyl Pyrrole-1-carboxylate
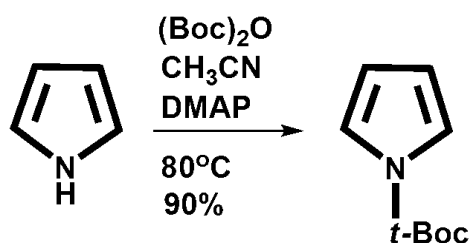
Figure 2. 3 Synthetic route for N-tert-Butyl Pyrrole-1-carboxylate

Di-tert-butyl dicarbonate, (Boc)$_2$O, (7.8 g, 35.7 mmol) and 4-dimethylamino)pyridine, DMAP, (0.5 g, 4.49 mmol) were added to pyrrole (2.0 g, 29.8 mmol) in acetonitrile (30 mL) under argon. After the addition was completed, the mixture was stirred at room temperature for two hours. Evaporation of the solvent and subsequent column chromatography (Al$_2$O$_3$, hexane), afforded 4.73 g (90% yield) of tert-butyl pyrrole-1-carboxylate as a colorless liquid.

2.3.1.4 *N*-(*tert*-Butoxycarbonyl)-2 (trimethylstannyl) pyrrole
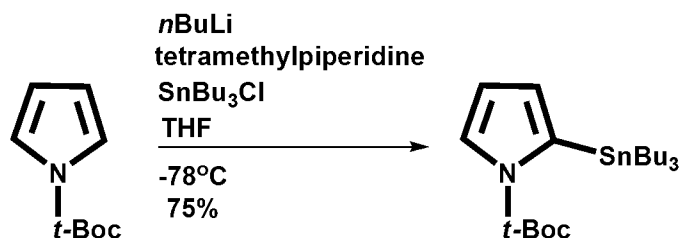
Figure 2. 4 Synthetic route for N-(tert-Butoxycarbonyl)-2 (trimethylstannyl) pyrrole

A 250-mL three-necked flask equipped with magnetic stirrer, a thermometer, a dropping funnel and nitrogen gas inlet was charged with dry THF (40 mL) and 2,2,6,6-tetramethylpiperidine (2.79 g, 19.75 mmol). The mixture was cooled to −78 °C and 18 mL of a 1.6 N solution of *n*BuLi (21.5 mmol) in hexane was added slowly so that the temperature of the mixture always remained below −65 °C. The mixture was stirred for 10 min at −75 °C, then warmed to 0 °C and stirred for additional 10 min. At this point, the mixture was cooled again to −75 °C and a solution of *tert*-butyl pyrrole-1-carboxylate (3 g, 17.94 mmol) in dry THF (40 mL) was added while keeping the temperature below −65 °C. The mixture was stirred for additional 90 min while keeping the temperature below −65 °C. A solution of Bu$_3$SnCl (7.5 mL, 23.32 mmol) in dry THF (40 mL) was added dropwise to the reaction mixture. The reaction was stirred for 40 min at −75 °C and additional 40 min at 0 °C and then for 12 h at room temperature. After removal of the THF under reduced pressure, water (50 mL) and diethyl ether (50 mL) were added to the crude and the aqueous phase was extracted with three

portions of diethyl ether. The combined organic layers were dried (MgSO$_4$) and the solvent was evaporated under reduced pressure. Column chromatography (Al$_2$O$_3$, hexane) of the resulting oil afforded 6.18 g (75% yield) of as a yellow liquid.

2.3.1.5 tributyl(4-hexylthiophen-2-yl)stannane
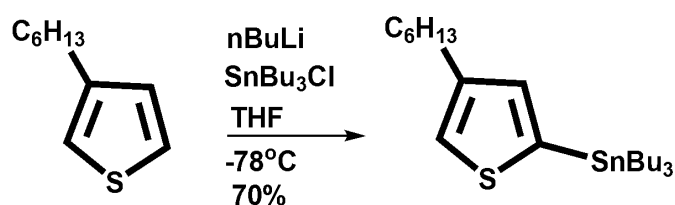
Figure 2. 5 Synthetic route for stannylation of 3-hexyl thiophene

3-Hexyl thiophene (4.7 g, 28.1 mmol) was dissolved in THF (80 mL), and the solution was cooled to -78$^{\text{o}}$C. n-Butyllithium (17.6 mL, 28.1 mmol) was added drop-wise, and the mixture was kept under stirring at -78$^{\text{o}}$C during 1 h. Then, tributyltin chloride (9.2 g, 28.1 mmol) was added at -78$^{\text{o}}$C via a syringe and the mixture was allowed to warm to room temperature with stirring for 24 h. At the end of the reaction, water (100 mL) was added to the mixture. The phases were separated and organic layer was extracted from the aqueous layer with CH$_2$Cl$_2$. All the organic layers were then washed with water, subsequently dried over MgSO$_4$ and concentrated to give product as a brown viscous liquid (70%).

2.3.1.6 2-Dodecyl-4,7-di(N-(tert-butoxycarbonyl)-2-pyrrolyl)-2Hbenzo[d] [1,2,3] triazole
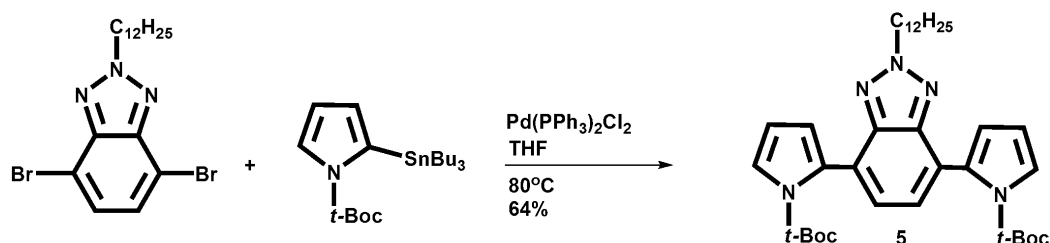
Figure 2. 6 Synthetic route for 2-dodecyl-4,7-di(N-(tert-butoxycarbonyl)-2-pyrrolyl)-2H-benzo[d][1,2,3]triazole

4,7-Dibromo-2-dodecyl-2H-benzo[d][1,2,3]triazole (445 mg, 1.0 mmol), and N-(tert-butoxycarbonyl)-2-(tributylstannyl) pyrrole (2.29 g, 5.0 mmol) were dissolved in anhydrous THF (150 ml) and purged with argon for 30 min. Then, dichlorobis(triphenyl phosphine)-palladium(II) (75 mg, 0.068 mmol) was added at room temperature under argon atmosphere. The mixture was refluxed for 3 days. Solvent was evaporated under vacuum and the crude product was purified by column chromatography on neutral alumina (eluent DCM:hexane, 2:1 v/v) to obtain 265 mg (64%) of 2-dodecyl-4,7-di(N-(tert-butoxycarbonyl)-2-pyrrolyl)-2H-benzo[d][1,2,3] triazole.

31

2.3.1.7 2-Dodecyl-4,7-di(1H-pyrrol-2-yl)-2Hbenzo[d][1,2,3]triazole (PyBT)
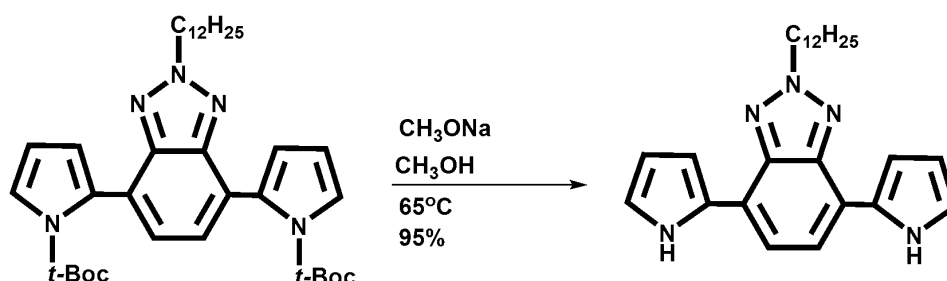
Figure 2. 7 Synthetic route for desired monomer PyBT

2-Dodecyl-4,7-di(N-(tert-butoxycarbonyl)-2-pyrrolyl)-2H-benzo[d][1,2,3] triazole. (200 mg, 0.48 mmol) was dissolved in 60 ml methanol. 120 mg Na, (5.2 mmol) were added and the reaction mixture was heated under reflux for 24 h. The solvent was evaporated and the residue was treated with water and extracted with dichloromethane. The organic extracts were dried over $MgSO_4$, the solvent was evaporated and the residue chromatographed on a column with silica gel using hexane: DCM (2:1 v/v) as eluent. 144 mg (95 %) PyBT was isolated.

2.3.1.8 2-Dodecyl-4,7-bis(4-hexylthiophen-2-yl)-2Hbenzo[d][1,2,3]triazole (HTBT)
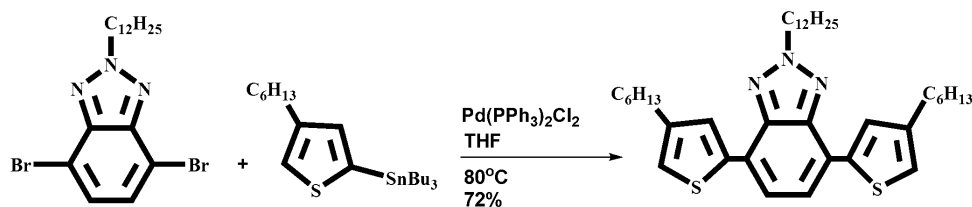
Figure 2. 8 Synthetic route for desired monomer HTBT

4,7-Dibromo-2-dodecylbenzotriazole (100 mg, 0.224 mmol), and tributyl(4-hexylthiophen-2-yl)stannane (511 mg, 1.12 mmol) were dissolved in THF (100 ml) and dichlorobis(triphenylphosphine)-palladium(II) (50 mg, 0.045 mmol) was added at room temperature. The mixture was refluxed for 12 hours under argon atmosphere. Solvent was evaporated under vacuum and the crude product was purified by column chromatography on silica gel to obtain 95 mg (72 %) HTBT.

2.4 Chemical and Electrochemical Polymerization of PyBT and HTBT
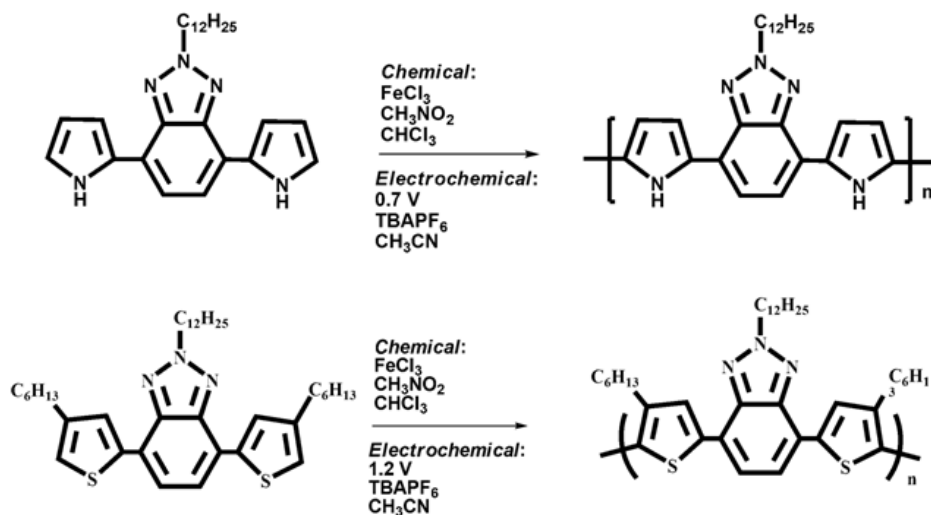
Figure 2. 9 Polymerization of PyBT and HTBT

150 mg of monomer (for both procedures) was dissolved in 20 mL of $CHCl_3$ under argon atmosphere. $FeCl_3$ (156 mg) in 20 mL of nitromethane slowly added to the monomer solution. Mixture was stirred for 12 h and then added into 200 mL methanol. The precipitate was filtered, dissolved in $CHCl_3$ and extracted with water. Solvent was removed and residue was dissolved in 50 mL THF and 50 mL hydrazine monohydrate: water (1:1) was added. In order to reduce the polymer to neutral form, mixture was stirred for 12 h. THF was evaporated under reduced pressure. Chloroform was added and organic phase was separated. Solvent was evaporated and the residue was stirred in acetone to remove unreacted monomers. The polymer was filtered and dried under vacuum. The resultant polymer was orange solid for PHTBT and purple for PPyBT. For electrochemical polymerization, anodic electropolymerization of the monomers

were performed in acetonitrile (ACN) with 0.1 M TBAPF$_6$ (tetrabutylammonium hexafluorophosphate) supporting electrolyte. ITO coated glass slides, Pt wire and Ag wire were used as working, counter and pseudo reference electrodes, respectively.

2.5   Characterization of The Polymers

2.5.1   Cyclic Voltammetry (CV)

Cyclic voltammetry is a convenient way of analyzing the electroactivity of monomers and obtaining the oxidation-reduction peak potentials of the polymers. CV scans linearly the potential of a stationary working electrode using a triangular waveform (Figure 2.10). During the potential sweep, the current resulting from the applied potential is measured by a potentiostat. Expected response of a reversible redox couple during a single potential cycle is given in Figure 2.11.
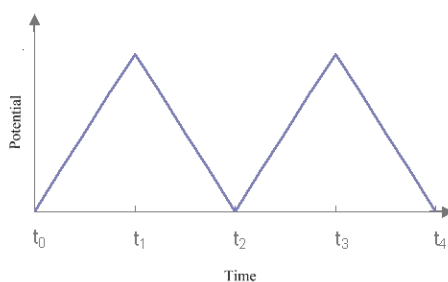
Figure 2. 10 Cyclic voltammetry waveform
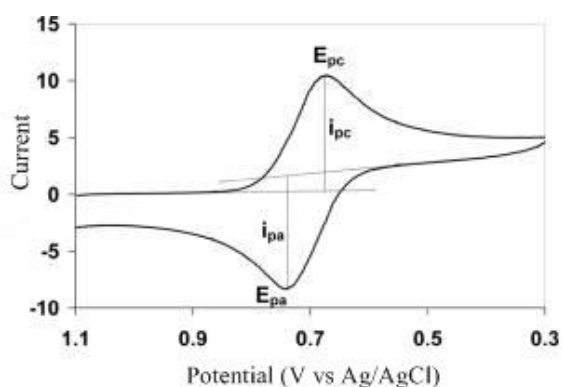
Figure 2. 11 A cyclic voltammogram for a reversible redox process

The characteristic peaks in the CV are formed due to the diffusion layer near the electrode surface. The resulting current peak reflects the continuous change of concentration gradient with time. Hence, the increase in the current corresponds to the achievement of diffusion control, while current drop (beyond the peak) is independent of the applied potential.

The peak height, i_p, is directly proportional to the concentration, C, as described by the Randles-Sevcik equation:

$$i_p = 0.4463 \ n \ F \ A \ C \ (n \ F \ v \ D \ / \ R \ T)^{1/2}$$

In this equation, n is the number of electrons appearing in half-reaction for the redox couple, v is the rate at which the potential is swept (V / sec), F is Faraday's constant (96485 C / mol), A is the electrode area (cm^2), R is the universal gas constant (8.314 J / mol K), T is the absolute temperature (K), and D is the analyte's diffusion coefficient (cm^2/sec). Note that if the temperature is assumed to be 25°C (298.15 K), the Randles-Sevcik equation can be written in a more concise form,

$$i_p = (2.687 \times 10^5) \, n^{3/2} \, v^{1/2} \, D^{1/2} \, A \, C$$

The Randles-Sevcik equation predicts that the peak current should be proportional to the square root of the sweep rate. For these processes, it was assumed that the reactants and products are soluble in solution and the surface processes (adsorption of reactants and products) can be neglected.

To study the electrochemistry of a polymer, a monomer free system should be used. The polymer redox process is quasi-reversible and since the polymer is immobilized at the electrode surface, the redox process is not diffusion controlled. Thus, under these circumstances Randles & Sevcik equation is no longer valid. Instead, according to the theory of immobilized redox centers, the peak current is given by;

$$i_p = n^2 F^2 \, \Gamma \, v \, / 4RT$$

where Γ is the total amount of reactant initially present at the electrode surface. According to this equation the current peak depends linearly on scan rate. Thus, investigation of peak current intensity with respect to scan rate will indicate the nature of electrochemical process as being diffusion controlled or whether the polymer is well adhered to the electrode surface or not.

2.5.2 Spectroelectrochemistry

Spectroelectrochemistry is a powerful tool to probe unique species that are generated in-situ during redox reactions at electrode surfaces, by the combination of electrochemical and spectroscopic techniques that can be operated at the same time. During redox switching of conjugated polymers, changes in electronic transitions occur which lead to changes in absorbance.

These changes make conjugated polymers useful in electrochromic applications such as smart windows, mirrors, etc. UV-Vis spectroscopy is used to monitor these electronic transitions. Spectra are recorded while the polymer is oxidized by increasing the potential stepwise. Spectroelectrochemistry experiments reveal some important properties of conjugated polymers such as band gap (E_g), λ_{max}, and the intergap states that appear upon doping like evolution of polaron and bipolaron bands. Similar studies were accomplished for electrochromic devices in order to investigate the spectral variations.

In order to probe electronic transitions upon doping-dedoping processes, spectral changes were investigated by UVvis- NIR spectrophotometer in a monomer free, 0.1 M TBAPF$_6$, ACN solution. Applied potentials were increased from -0.5 to 1.0 V for PPyBT and from -0.5 V to 1.1 V for PHTBT where these polymers were coated on ITO glass slides potentiodynamically.

2.5.3 Kinetic Studies

Electrochromic switching studies are performed to monitor the percent transmittance changes as a function of time and to determine the switching time of the polymer at its λ_{max} by stepping potential repeatedly between the neutral and oxidized states. A square wave potential step method coupled with optical spectroscopy known as chronoabsorptometry was used to investigate switching times and contrast in the polymer.

In order to study switching properties of polymers, PPyBT and PHTBT were deposited on ITO-coated glass slides as thin films via potentiodynamic electrolysis in a 0.1 M TBAPF$_6$ and 1×10^{-2} M monomer solution in acetonitrile (ACN) at a scan rate of 100 mV/s.

Square-wave potential utilized to polymer coated ITO slides in a monomer free TBAPF$_6$/ACN electrolyte solvent couple, between fully reduced states of polymers to fully oxidized states with a residence time of 5 seconds.

2.5.4 Colorimetry

Colorimetry analysis was performed to determine three attributes used to describe the color: hue, saturation and brightness. Hue represents the wavelength of maximum contrast (dominant wavelength) and is commonly referred to color. Saturation represents the purity (intensity) of the color, whereas the third attribute, brightness, deals with the luminance of the material, which is the transmittance of light through a sample as seen by the human eye.

A commonly used scale that numerically defines colors was established in 1931 by The Commission Internationale de l'Eclairge (CIE system) with L*a*b, CIE color spaces. Color measurements were performed via Coloreye XTH Spectrophotometer.

2.5.5 Gel Permeation Chromatography (GPC)

Average molecular weight was determined by gel permeation chromatography (GPC) using a Polymer Laboratories GPC 220 calibrated with universal standard Polystyrene. In order to determine the average molecular weights (M_n & M_w), 5 mg of polymers were dissolved in THF.

2.6   Characterization of The Solar Cells

I-V characteristics of the devices were measured in the dark and under illumination from a Steuernagel solar simulator (with a metal halogen lamp as light source with an AM 1.5 filter) under an illumination density of 100 mW cm^{-2} calibrated using a standard silicon diode, respectively. The I-V curves were measured with a Keithley SMU 236. ITO was connected to the positive electrode, Al to the negative. The curves were recorded by continuously sweeping from –2V to +2V and recording data points in 10 mV steps. The spectral photocurrent was detected by a EG&G Instruments 7260 Lock-in amplifier. The sample was illuminated with monochromatic light of a Xenon lamp. The spectrum of the light source was measured each time with a calibrated monocrystalline silicon diode.

CHAPTER 3

RESULTS AND DISCUSSION

3.1   Characterization

^{1}H-NMR, ^{13}C-NMR spectra of monomers were investigated in $CDCl_3$ and chemical shifts (δ) were given relative to tetramethylsilane as the internal standard.

3.1.1   2-Dodecylbenzotriazole

[1]H (400 MHz, $CDCl_3$, δ): 7.76 (m, 2H), 7.26 (m, 2H), 4.62 (t, J) 7.1 Hz 2H), 2.12 (m, 2H), 1.25-1.15 (m, 18H), 0.78 (t, J) 6.0 Hz, 3H). ^{13}C NMR (100 MHz, $CDCl_3$, δ): 144.3, 126.1, 117.9, 56.6, 31.8, 30.0, 29.5, 29.4, 29.4, 29.3, 29.3, 29.0, 26.5, 22.6, 14.0.
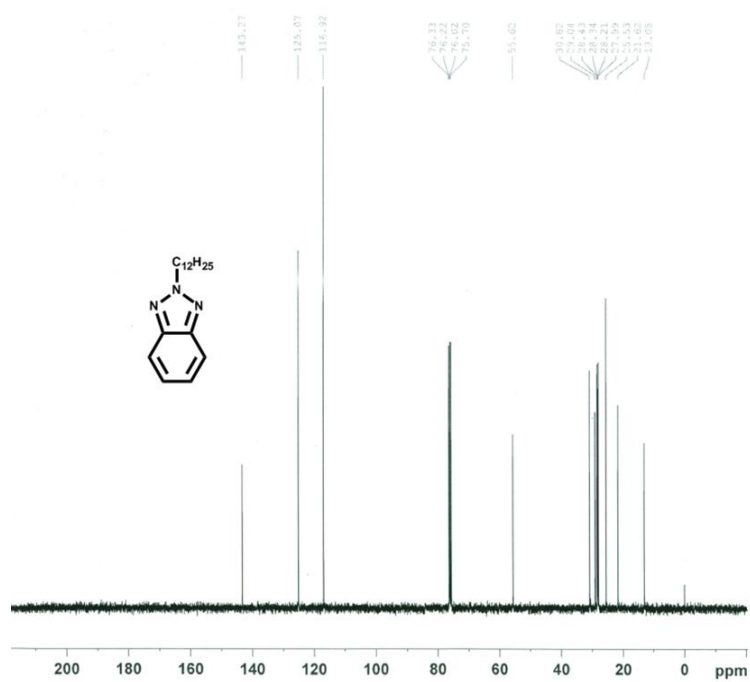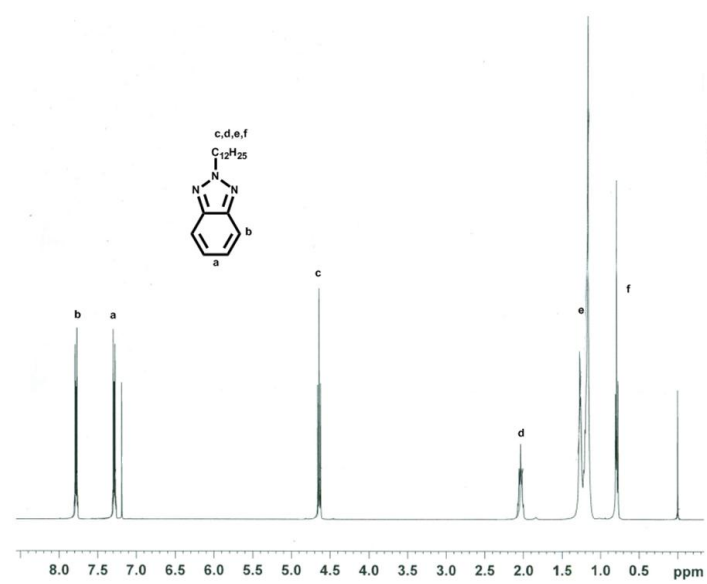
Figure 3. 1 ¹H-NMR and ¹³C NMR of 2-dodecylbenzotriazole

3.1.2 4,7-Dibromo-2-dodecylbenzotriazole

^{1}H (400 MHz, CDCl3, δ): 7.36 (s, 2H), 4.60 (t, J) 7.0 Hz, 2H), 2.10 (m, 2H), 1.38-1.12 (m, 18H), 0.80 (t, J) 6.9 Hz, 3H). ^{13}CNMR (100 MHz, CDCl3, δ): 143.7, 129.4, 109.9, 57.4, 31.8, 30.1, 29.5, 29.5, 29.4, 29.4, 29.3, 28.9, 26.4, 22.6, 14.0.
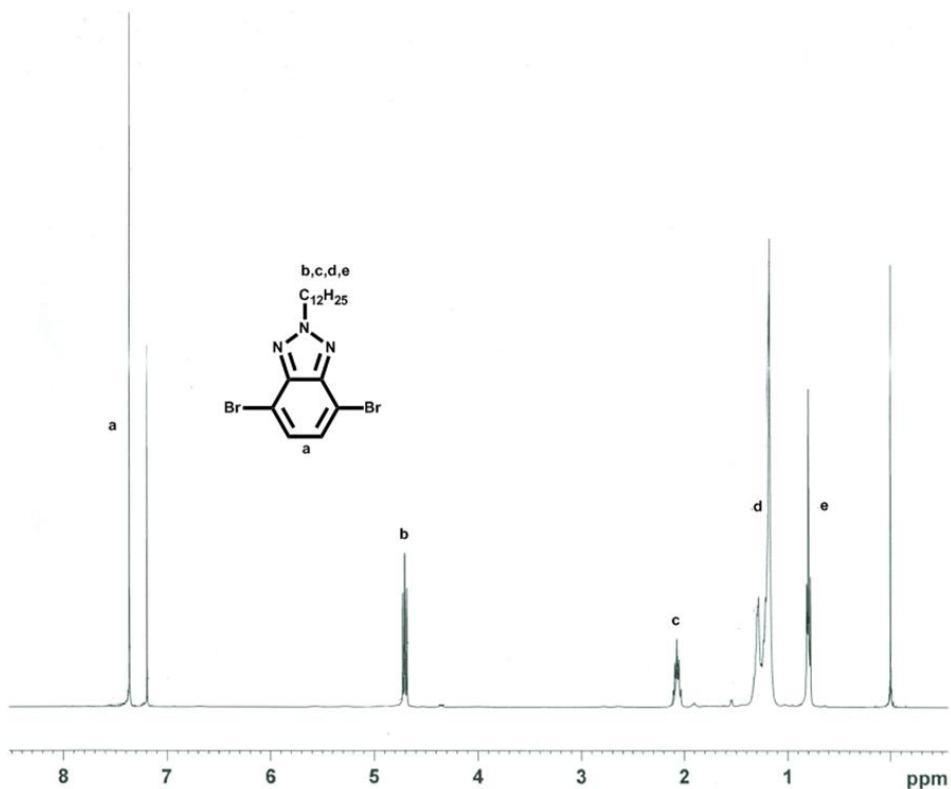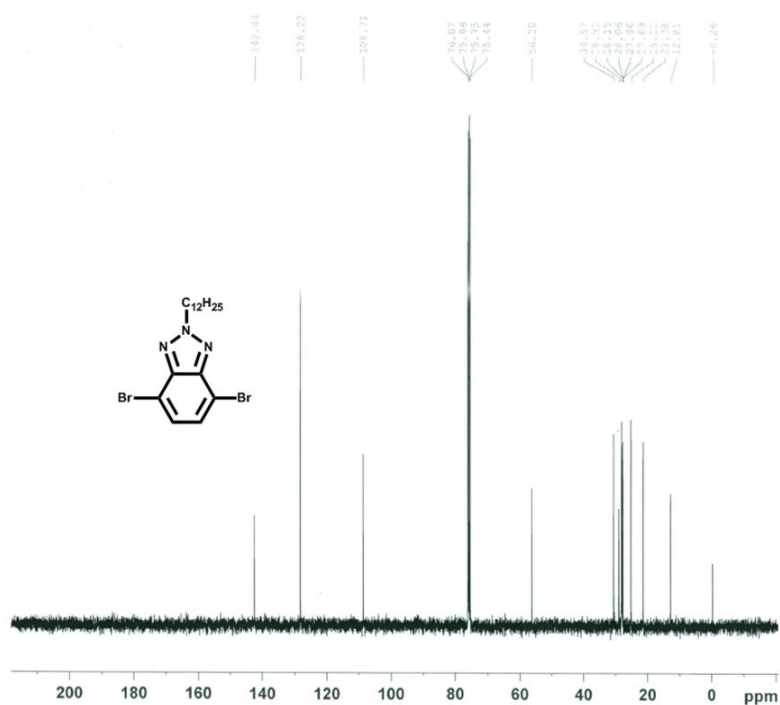
Figure 3. 2 ^{1}H-NMR and [13C] NMR of 4,7- Dibromo-2-dodecylbenzotriazole

3.1.3 2-Dodecyl-4,7-di(N-(tert-butoxycarbonyl)-2-pyrrolyl)-2Hbenzo[d] [1,2,3] triazole

[1]H (400 MHz, CDCl$_3$, δ): 7.43 (d, 2 H, J = 8.4 Hz), 7.12 (s, 2H), 6.32 (d, 2H, J = 7.0 Hz), 6.26 (t, 2H,J = 6.4 Hz), 4.52 (t, J = 7.1 Hz 2H), 2.02 (m, 2H), 1.25-1.15 (m, 18H), 0.78 (t, J = 6.0 Hz, 3H). [13C] NMR (100 MHz, CDCl$_3$, δ): 149.5, 143.9, 131.1, 125.0, 124.5, 123.5, 115.6, 111.04, 83.45, 56.3, 31.8, 30.1, 29.5, 29.5, 29.4, 29.4, 29.3, 28.9, 26.4, 22.6, 14.0.
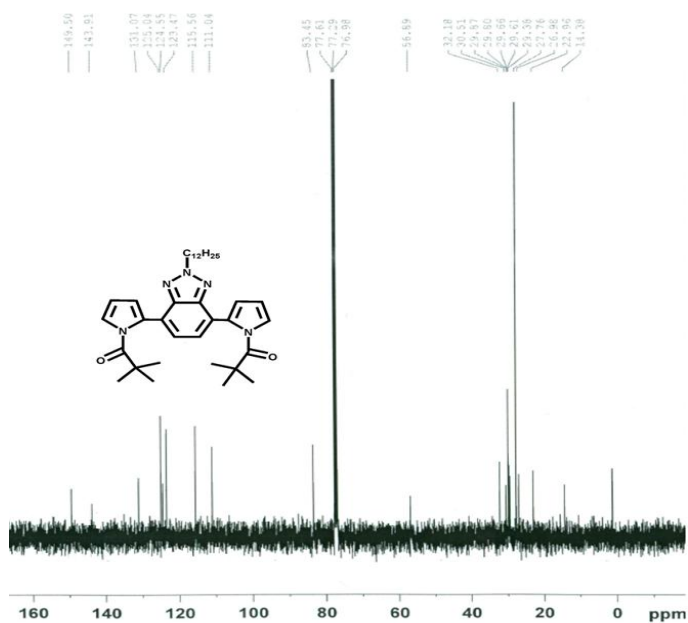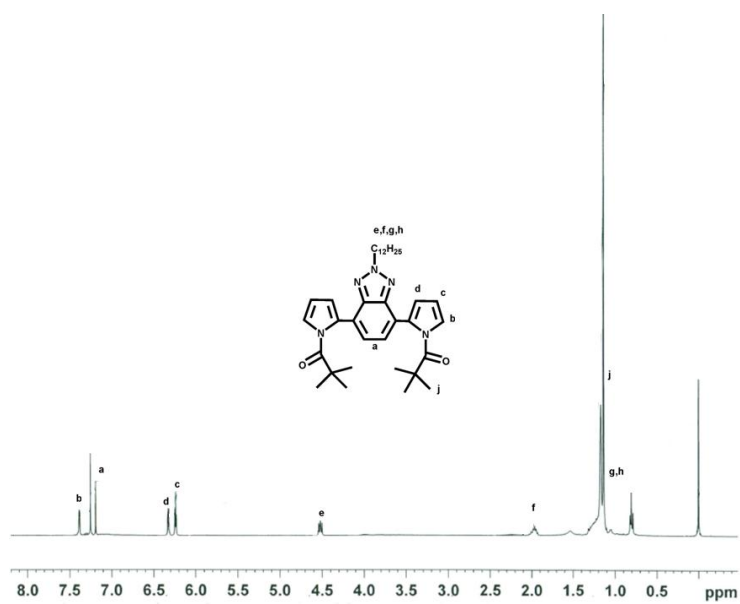
Figure 3.3 ¹H-NMR and ¹³C NMR of 2- Dodecyl-4,7- di(N-(tert-butoxy carbonyl)-2-pyrrolyl)-2H-benzo[d][1,2,3]triazole

45

3.1.4 2-Dodecyl-4,7-di(1H-pyrrol-2-yl)-2Hbenzo[d][1,2,3]triazole (PyBT)

[1]H (400 MHz, CDCl$_3$, δ): 10.42 (s, 2H), 7.66 (s, 2 H), 6.90 (d, 2H, J = 7.0 Hz), 6.75 (d, 2H, J = 6.8 Hz), 6.32 (t, 2H, J = 6.4 Hz), 4.62 (t, J = 7.1 Hz 2H), 2.02 (m, 2H), 1.25-1.15 (m, 18H), 0.78 (t, J = 6.0 Hz, 3H). ^{13}C NMR (100 MHz, CDCl$_3$, δ): 139.0, 127.4, 117.4, 116.8, 116.7, 107.5, 103.4, 54.35, 30.0, 29.5, 29.4, 29.4, 29.3, 29.3, 29.0, 26.5, 22.6, 14.0.
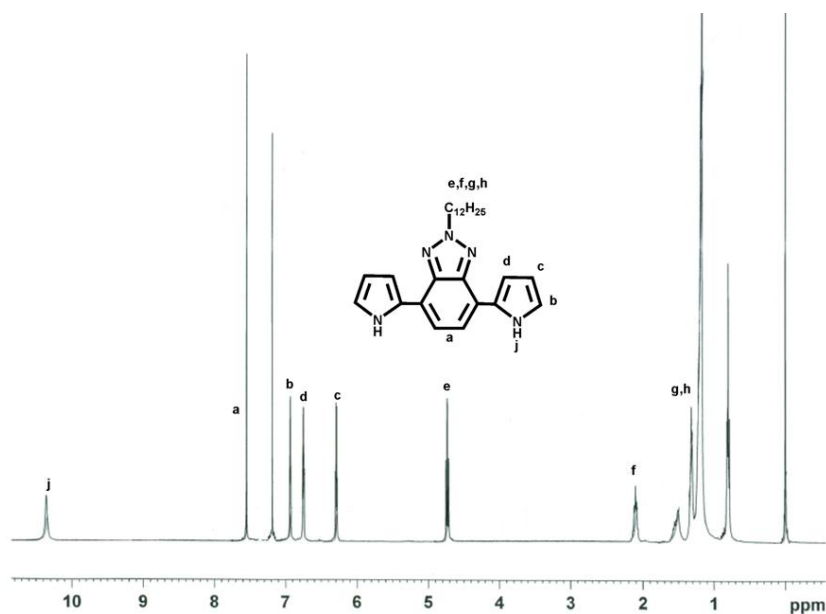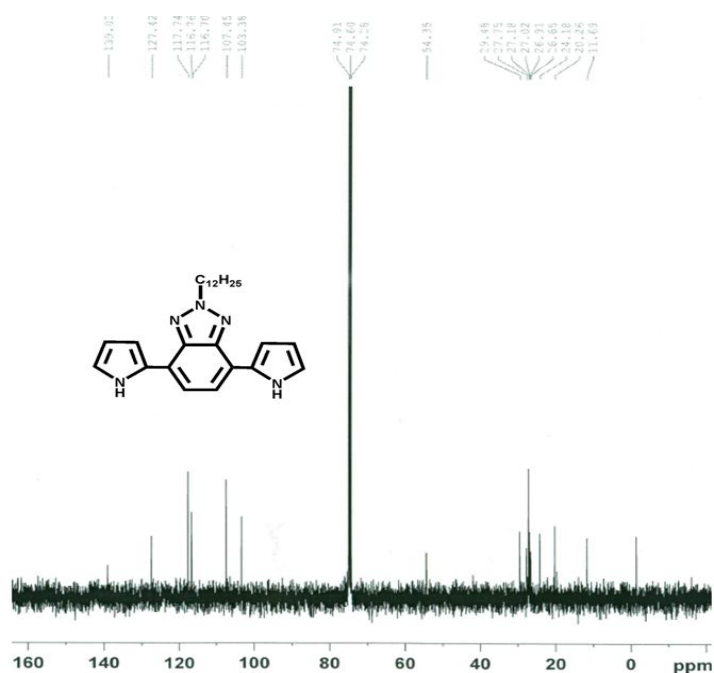
Figure 3.4 ¹H-NMR and ¹³C-NMR of 2-Dodecyl-di(1H- pyrrol-2-yl)-2Hbenzo[d] [1,2,3] triazole (PyBT)

3.1.5 2-Dodecyl-4,7-bis(4-hexylthiophen-2-yl)-2Hbenzo[d][1,2,3]triazole (HTBT)

¹H NMR (400MHz, CDCl₃,): 7.9 (s, 2H), 7.5 (s, 2H), 6.9 (s,2H), 4.8 (t, J=7.0 Hz, 2H), 2.1 (m, 2H), 1.4-1.1 (m, 18H), 0.9 (t, J=6.9 Hz, 3H); ¹³C NMR (100 MHz, CDCl₃,): 143.1, 140.1, 138.3, 127.1, 122.4, 121.3, 119.0, 55.5, 30.6, 30.5, 29.5, 29.2, 28.8, 28.4, 28.2, 27.8, 25.49, 21.4, 12.8 MS (m/z): 619 [M+]

47
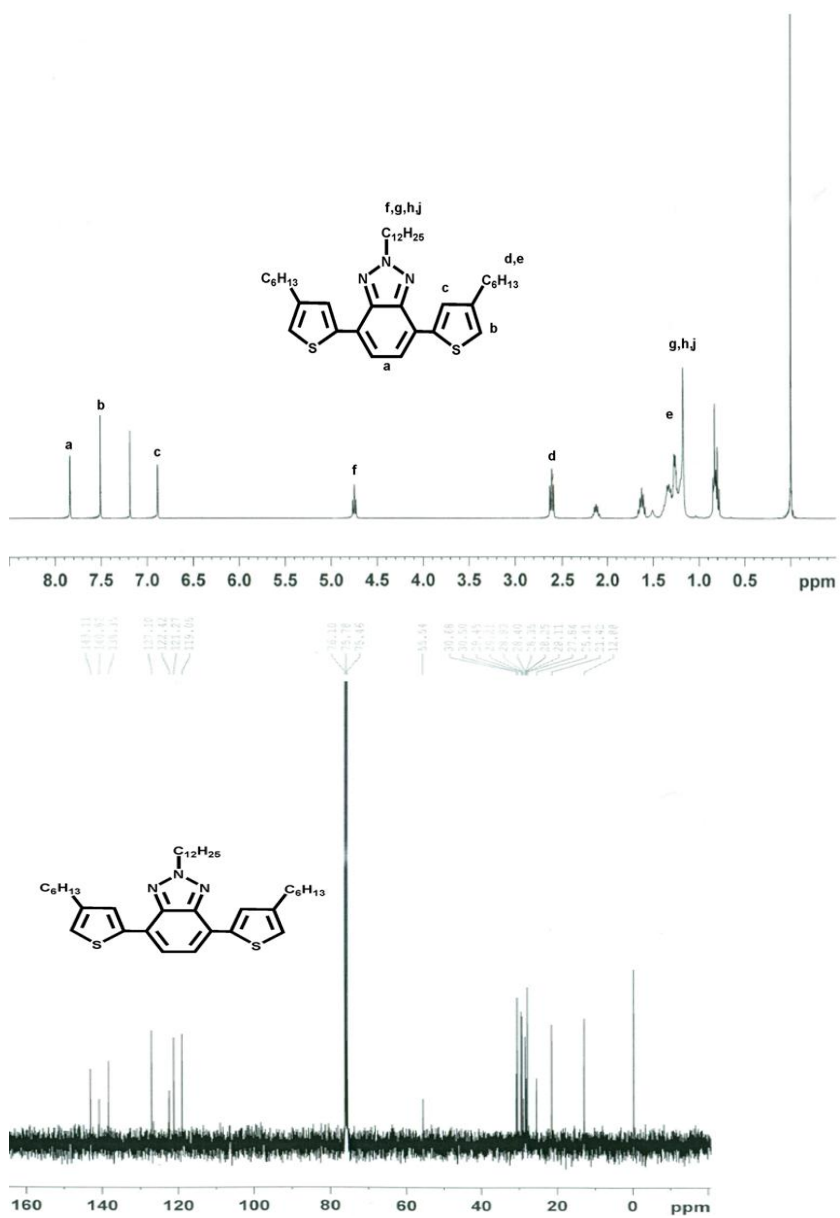
Figure 3. 5 ¹H and ¹³C-NMR of 2-Dodecyl-(4,7-bis(4-hexylthio phen-2-yl) -
2Hbenzo[d] [1,2,3]triazole (HTBT)

3.2 PyBT

3.2.1 Cyclic Voltammetry (CV)

In order to work out the redox behavior of PyBT in detail, cyclic voltammetry (CV) studies were carried through in a 0.1 M $TBAPF_6$/ACN solution. As described in Figure 3.6, PyBT shows an oxidation peak at 0.7 V accompanied by a reversible redox couple at 0.2 V and 0.4 V versus Ag/AgCl quasi reference electrode. During repetitive cycles, increase in current densities confirmed the formation of an electroactive polymer film on the ITO glass. Using cyclic voltammogram of PyBT, oxidation-to-reduction peak ratios were calculated as very close to 1.0, which is a prominent indication for superior reversibility of the redox process. PyBT showed a significant decrease in monomer oxidation compared to other benzotriazole containing donor acceptor type molecules.[50,67] This property can be attributed to the donor-acceptor match capacity of benztriazole and pyrrole units.
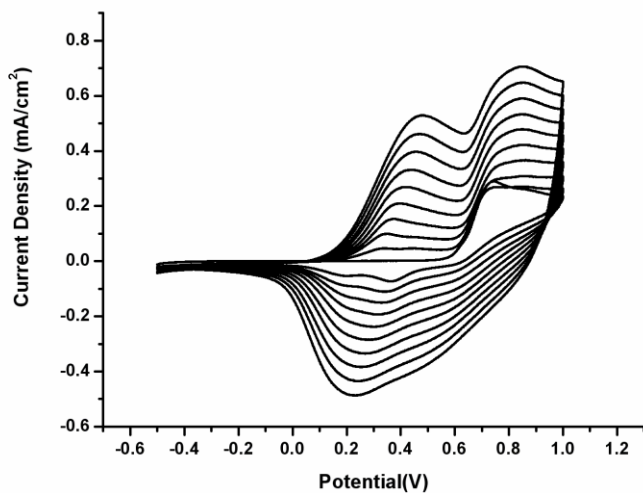
Figure 3. 6 Electropolymerization of PyBT on ITO in 0.1 M TBAPF$_6$ /ACN electrolyte-solvent couple at a scan rate of 100mV/sec.

Figure 3.7 clearly illustrates the redox behavior of the polymer film investigated in monomer free solution, using TBAPF$_6$/ACN solvent-electrolyte system. A true linear relationship between peak response and scan rate indicated a non-diffusion controlled redox process and a well adhered electroactive polymer film.
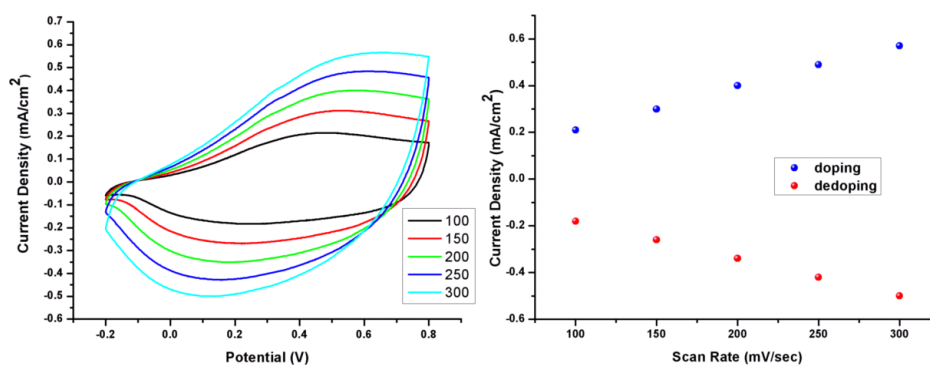
Figure 3. 7 Scan rate dependence (a) and linear relationship between scan rate and current density (b) of PPyBT film on ITO glass slides in monomer free TBAPF$_6$ /ACN system.

The unique acceptor capacity of benzotriazole with pyrrole led PPyBT to be n-type dopable. In literature, it is stated that due to the increase in sensitivity in the reduced form, pyrrole containing polymers are usually impossible to n-type doping. [68] We have overruled this bias using benzotriazole in D-A-D system. Figure 3.8 exhibits a single scan cyclic voltammogram of the polymer film under open air atmosphere in a 0.1 M TBAPF$_6$/ACN solution. During reduction of the polymer, a reversible redox couple at -1.67 V and -1.05 V of the polymer film was observed confirming the n-doping process.
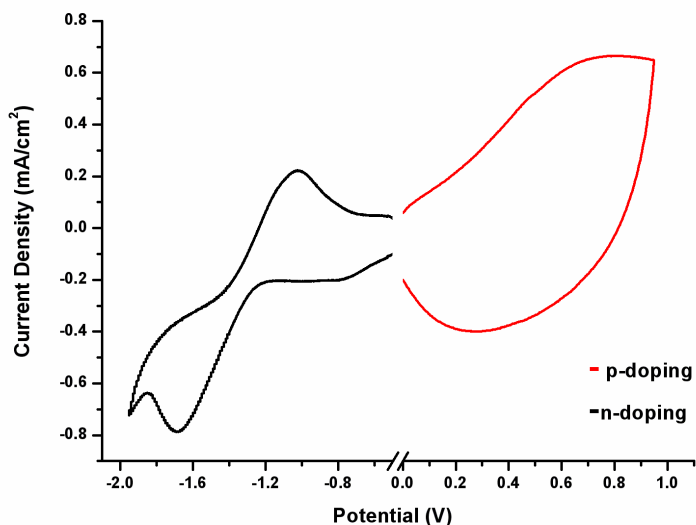
Figure 3. 8 Single scan cyclic voltammogram of pristine polymer film of PPyBT for both p-and-n type doping under open air atmosphere.

Oxidation-reduction onset values of PPyBT were determined from cyclic voltammetry (CV). Hence, HOMO-LUMO values for the polymer were estimated from electrochemical data (Table 1). From CV experiments, the HOMO and LUMO levels of PPyBT were estimated as -4.95 and -3.40 eV, respectively (the value of NHE was used as -4.75 eV throughout the study [69]). The energy levels versus vacuum level were calculated according to the following equations:

$E_{HOMO} = - (E_{onset,ox} + 4.75)$ (eV)

$E_{LUMO} = - (E_{onset,red} + 4.75)$ (eV)

$E^{ec} = (E_{onset,ox} - E_{onset,red})$ (eV) where by $E_{onset,ox}$ and $E_{onset,red}$ represent the onset oxidation and reduction potentials, respectively. The band gap values determined from both CV and spectroelectrochemistry were in good agreement.

Table 1 Cyclic Voltammetry results of PHTBT (CV was recored in 0.1 M ACN/ TBPF$_6$ at 100 mV/s scan rate)

PPyBT	Oxidation potential (V)		Reduction Potential (V)		Bandgap (eV)		Energy Level (eV) From CV	
	E_{ox}	$E_{onset,ox}$	E_{red}	$E_{onset,red}$	Eg^{ec}	Eg^{op}	HOMO	LUMO
	0.40	0.20	-1.67	-1.35	1.55	1.65	-4.95	-3.40

3.2.2 Spectroelectrochemistry

To investigate the spectral changes upon doping and dedoping processes, PPyBT was characterized in monomer a free solution in conjunction with TBAPF$_6$/ACN solvent-electrolyte system, using UV-vis-NIR spectrophotometry. Figure 3.9 demonstrates the change in the electronic absorption spectra of PPyBT upon increasing potentials between 0 V and +1.0 V. In the neutral form, the polymer shows a well defined absorption maxima at 332 nm and 577 nm with a deep purple color (Y: 32.2 x: 0.25 y: 0.24). These two maxima are π-π* transitions due to the donor-acceptor nature of the polymer backbone. [70]
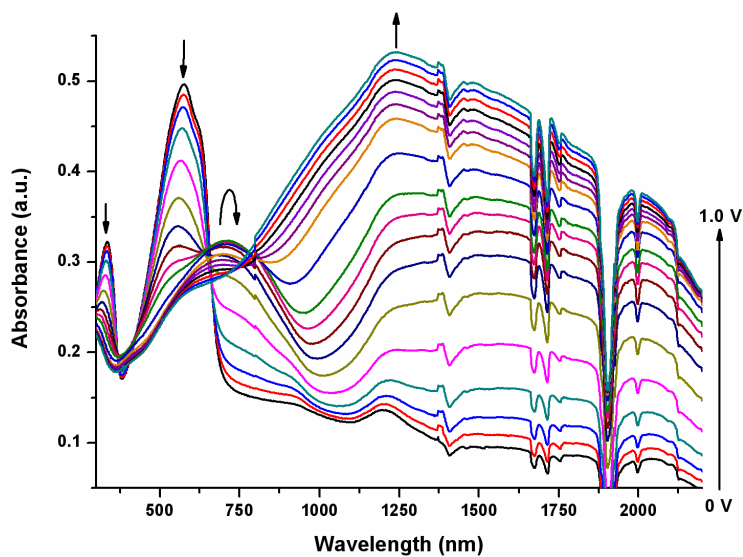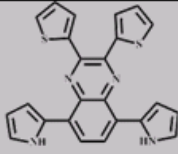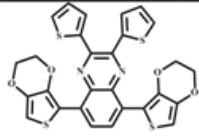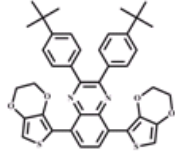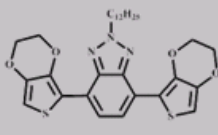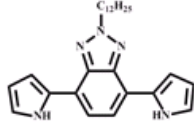
Figure 3. 9 Change in the electronic absorption spectra of PPyBT at potentials between 0 V and +1.0 V with 0.05 V potential intervals.

It is striking that, PPyBT is purple in its neutral form, goes through a blue absorbing state (Y: 55.5 x: 0.27 y: 0.31) when partially oxidized, and finally becomes highly transparent in its fully oxidized state. At low doping levels, the absorption bands at 332 nm and 577 nm decreased simultaneously and two new absorption maxima in the visible and NIR regions at 700 nm and 1230 nm intensified as a result of the charge carriers such as polaronic and bipolaronic bands, respectively.[71] Upon further oxidation of the polymer film, the bands in the UV-vis regions reach a minimum value and the band at 700 nm starts to decrease due to the conversion of radical cations to dications on the polymer backbone which leads to a highly transmissive color (Y: 67.6 x: 0.29 y: 0.32) in the visible region. The optical band gap of PPyBT was calculated from the low energy transition as 1.65 eV which can be regarded as a low band gap material

54

among conjugated polymers.[72] Although pyrrole is used as donor group in PPyBT case, the colors of the polymer film are very similar to PEDOT and EDOT containing counterparts.[63] Indeed, previous studies showed that no matter which donor group (EDOT or pyrrole) is used with an acceptor unit; the polymer exibits very similar characteristics. [73]

Table 2 summarizes various properties of such pyrrole and EDOT containing D-A-D groups synthesized previously. When quinoxaline moeities were used with EDOT as the donor; the green color, a necessity to complete the RGB system, was achieved in the neutral forms of the polymers. In a similar manner, pyrrole containing monomers with the same acceptor group revealed also green color in their reduced states. Although polypyrrole and PEDOT have different colors in their neutral states; polymers consisted of such units as the donor exhibited the same colors. This can be attributed to the similarity in donor-acceptor match between the acceptor units and either EDOT or pyrrole. Besides these, it is noteworthy to state that among others, PPyBT is the only one which is soluble when polymerized both electrochemically and chemically.

Table 2 The structures of pyrrole and EDOT based D-A-D type monomers and properties of their polymers.

	Emon,ox (V)	Lambda max (nm)	Optical Band gap(eV)	Solubility (X/√)	n-type character (X/√)
	0.7	400 815	1.0	X	X
	0.85	405 780	1.2	X	√
	0.54	408 745	1.25	X	X
	0.9	452 711	1.18	X	√
	0.97	618	1.6	X	X
	0.7	577	1.65	√	√

Conducting polymers with durable negatively doped states are of high interest due to the applicibality to more complex devices such as solar cells and LEDs. [74] To attain such significant property under ambient conditions makes these polymers more attractive to these studies. As stated previously by Reynolds et al., only a simple electrochemical reduction is not sufficient to prove the process to be n-type doping. [24b] In addition to reversible peaks observed in CV, conformation for charge carrier formation upon reduction should also be studied. Figure 3.10 reveals t he encouraging true n-doping behavior of PPyBT upon applied negative potentials. PPyBT film was coated potetiostatically for 2 min. until 5 mC charge was deposited on ITO (0.01 M monomer in 0.1 M TBAPF$_6$/ACN solution) since n-doping process can be achieved with thinner films. A drastic increase in absorption in the NIR region at negative potentials is a clear evidence for n-doping process. When reduced, polymer film shows a light blue color (Y: 70.3 x: 0.30 y: 0.31). As shown in Table 2, none of the pyrrole containing monomers are n-type dopable. It is improtant to state that low lying LUMO allows PPyBT to be n-dopable.
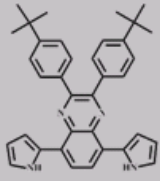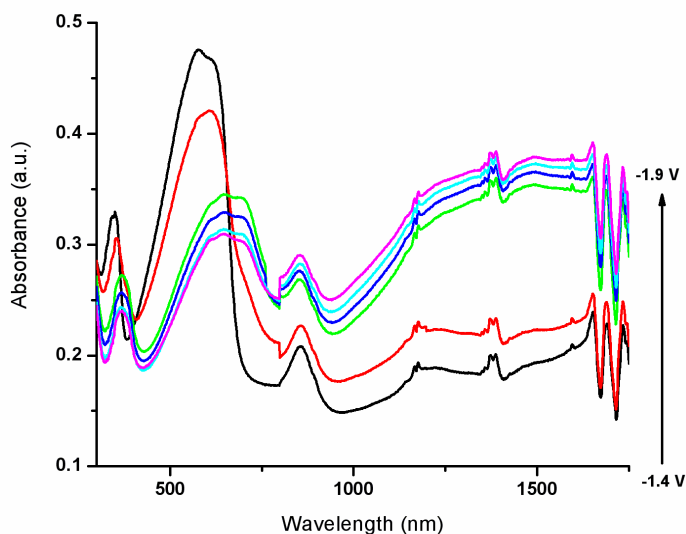
Figure 3. 10 Change in the electronic absorption of PPyBT upon reduction between -1.4 V and -1.9 V with 0.1 V potential intervals.

Coloration efficiency is the ratio between injected/ejected charge per unit area of the electrode and the change in optical density at a dominant wavelength. [75] The corresponding value at 577 nm was calculated as 256 cm^2/C for PPyBT.

3.2.3   Kinetic Studies

Chronoamperometry studies were performed to monitor the changes in transmittance as a function of time while sweeping the potentials between fully oxidized and reduced states and the switching abilities of the polymer film at its maximum absorption wavelengths. During the experiment, optical contrasts of the polymer film at corresponding wavelengths were recorded using a UV-vis-NIR spectrophotometer while the potential was switched between 0.0 V and +1.0 V in

5 s time interval. PPyBT revealed 30 % optical contrast between its neutral and oxidized states at 577 nm with a swithcing time of 0.5 s. In NIR region, polymer film showed 46 % transmittance change within 1.2 s which enables the PPyBT to be used in NIR applications (Figure 3.11).
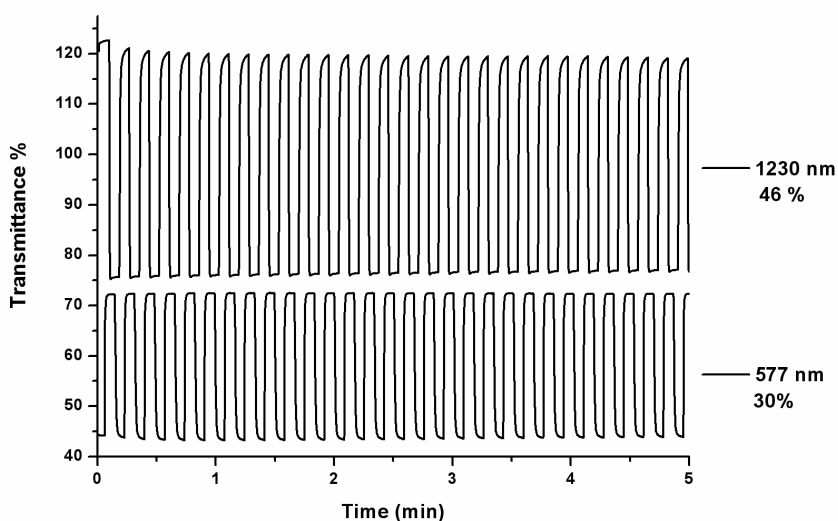
Figure 3. 11 Electrochromic switching and percent transmittance changes observed at 577 nm and 1230 nm for PPyBT upon switching between 0.0 V and + 1.2 V in 0.1 M TBAPF$_6$/ACN system.

To determine the long term switching ability of the polymer film, PPyBT was deposited on ITO coated glass using cyclic voltammetry with a solution of 0.01 M monomer and 0.1 M TBAPF$_6$/ACN solution. Apart from using cyclic voltammetry, chronoamperometry was studied to investigate the stability of PPyBT. Switching the polymer film between colored and bleached states rather

59

than increasing potential linearly resulted in more accurate results. Less than 10 % charge loss was observed after 1000 full switches of the polymer (between fully reduced and oxidized states) (Figure 3.12).
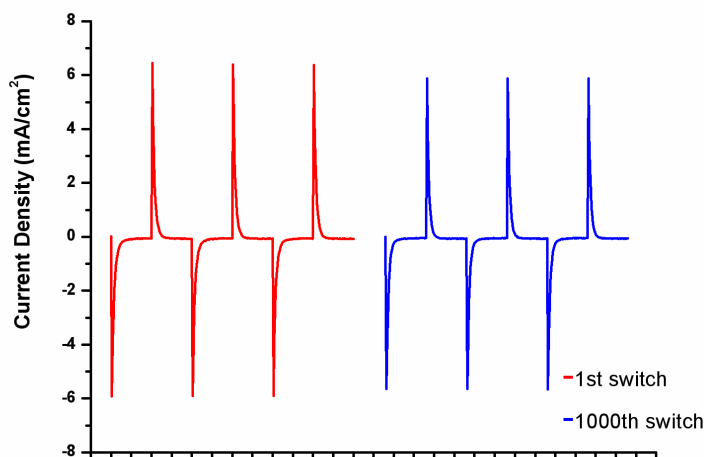
Figure 3. 12 Switching ability of the polymer film after 1000 full switches in 0.1 M TBAPF$_6$/ACN solvent-electrolyte system.

3.2.4 BHJ Solar Cell Fabrication and Characterization

In order to use PPyBT as a donor material in organic bulk heterojunction (BHJ) solar cells, it was chemically polymerized and mixed with PCBM as the acceptor. [79] The molecular weight of the chemically prepared polymer was found to be Mn:11900 and Mw: 30600. As determined from the CV measurements, PPyBT has an oxidation onset at 0.2 V and a reduction onset at -1.35 V vs. NHE resulting in a HOMO-LUMO level of -4.95 eV and -3.40 eV (assuming a value of -4.75 eV vs. vacuum level for NHE). The band energies of PCBM were estimated as -6.1eV and -4.3 eV for HOMO an LUMO, respectively.

(Figure 3.13) [80]There was enough difference (~0.3-0.4 eV) between LUMO of the donor and the acceptor in order to take place a charge transfer from photoexcited polymer to PCBM. [72]
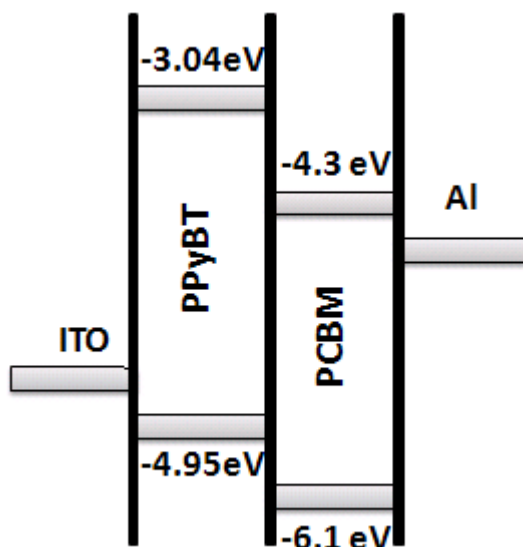
Figure 3. 13 Approximate HOMO-LUMO values for PPyBT and PCBM.

The photovoltaic devices were prepared from the blends of PPyBT and PCBM (1:2 and 1:3 w/w; 5mg PPyBT :10mg PCBM for 1:2 ratio) in a solution of chlorobenzene (CB). The dodecyl groups on the benzotriazole unit helped the polymer to be soluble in common organic solvents such as chloroform, THF and chlorobenzene. PPyBT showed a maximum absorption band centered at 577 nm in film form as stated in the spectroelectrochemistry part, which resulted in a purple color in its undoped; i.e. semiconductor state (Figure 3.14). Onto a poly(3,4 ethylenedioxythiophene) (PEDOT): poly(styrenesulfonate) (PSS) covered ITO glass slides, active layer (PPyBT: PCBM blends) was spin coated and aluminum (100 nm) was thermally evaporated as top electrode to achieve the layered stucture of bulkheterojunction solar cell.
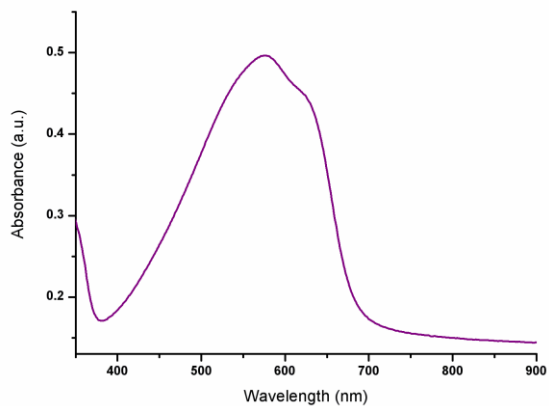
Figure 3. 14 Electronic absorption spectrum of pristine polymer film.

Charge transfer was confirmed by a quenched PL emission when adding 50 wt % PCBM (Figure 3.15). Such photoluminescence quenching can be the proof of a ultrafast photoinduced charge transfer from the PPyBT to PCBM. [81]
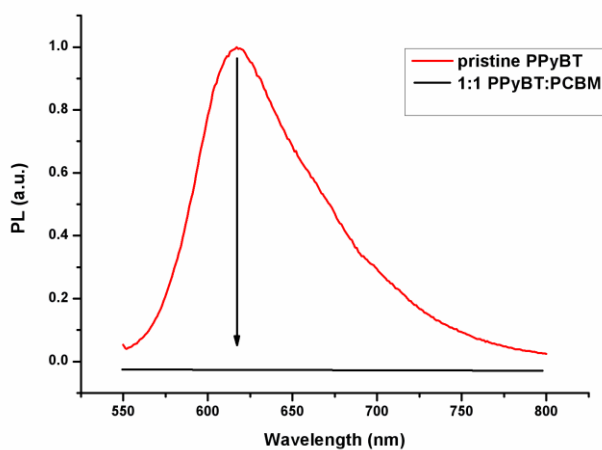
Figure 3. 15 PL quenching of PPyBT when mixed with 50 wt % of PCBM.

62

Photocurrent measurements showed that the PPyBT: PCBM blend can genarate electrons nearly over the range of the absorption spectrum of pristine polymer. The incident photon to current efficiency (IPCE) is used to acquire information on the number of photons of different energies that contributes the charge generation in the BHJ solar cell. [82]

In Figure 3.16, IPCE % plot spans from 350 to 900 nm and shows slightly over 3 % contribution at around 450 nm.
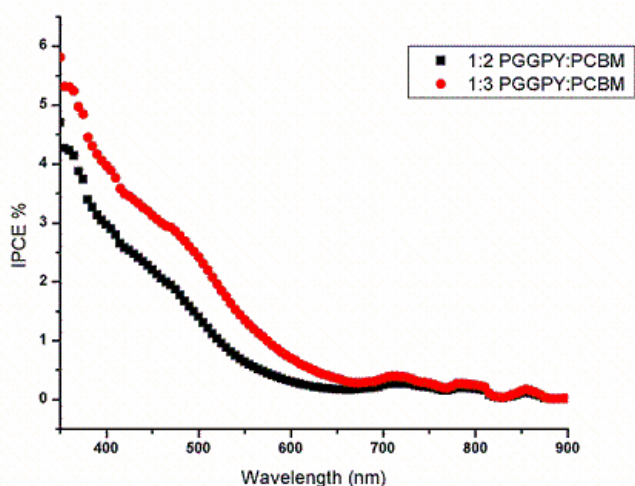
Figure 3. 16 IPCE % plots of PPyBT: PCBM blends of 1:2 and 1:3 (w:w).

The *I-V* characteristics of the solar cells in dark and under illumination of PPyBT:PCBM are shown in Figure 3.17.
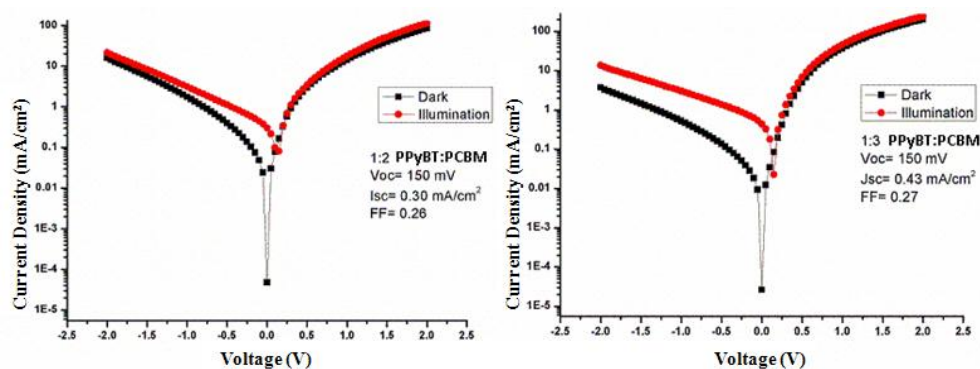
Figure 3. 17 Current-Voltage (*I-V*) characteristics of the PPyBT/PCBM blends of 1:2 and 1:3 in the dark and under white light illumination (AM 1.5 conditions) shown in semilogarithmic plot.

The BHJ devices under white light illumination (100 mWcm^{-2}) showed short circuit current densities (J_{sc}) of 0.3 mAcm^{-2} and 0.43 mAcm^{-2}, open circuit voltage (V_{oc}) of 0.15 V and fill factors of 0.26 and 0.27. The low rectification ratios can be attributed to the rather poor film formation of the active layer. It should be noted that PPyBT is one of the handful pyrrole bearing polymer used in bulk heterojunction solar cells. [83] Further optimizations of the devices by altering the parameters such as mixing ratios, light intensity and device construction conditions can be helpful to accomplish the detailed characterization of PPyBT as an effective low bandgap material for photovoltaic applications.

3.3 PHTBT

3.3.1 Cyclic Voltammetry (CV)

HTBT was polymerized potentiodynamically between 0.0 V and 1.4 V vs. Ag/AgCl quasi reference electrode in a 0.1 M acetonitrile (ACN)/tetrabutylammonium hexafluorophosphate (TBAPF$_6$) solution onto ITO coated glass slide in order to observe the polymer characteristics. During polymerization, a characteristic oxidation peak of monomer was observed at 1.2 V accompanied by a reversible couple for oxidation and reduction of the polymer. In Figure 3.18, the increase in current density with the number of scans clearly shows the deposition of an electroactive film of PHTBT on ITO. The resultant polymer was soluble in common organic solvents and revealed reversible both p and n doping properties where the p doping/dedoping were indicated by the peaks at 0.9 V and 0.5 V respectively. The PHTBT film is orange (Y: 60.1 x: 0.50 y: 0.47) in its neutral state and reveals blue color (Y: 23.0 x: 0.27 y: 0.30) when oxidized.
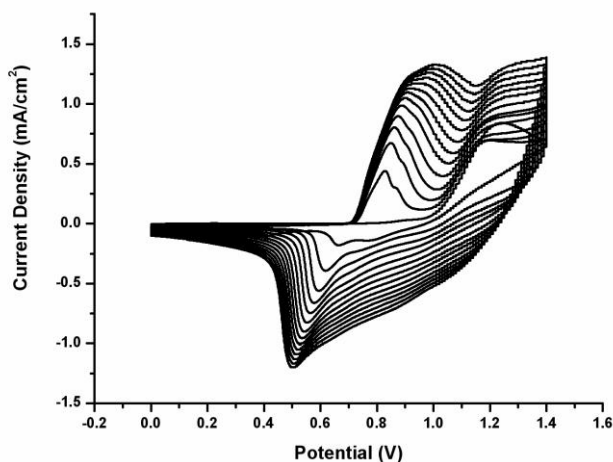
Figure 3. 18 Electrochemical deposition of PHTBT on ITO coated glass slide in a 0.1 M ACN/TBAPF$_6$ solvent-electrolyte couple.

Oxidation-to-reduction peak ratios were calculated from CV as almost 1.0, which is a clear indication for reversibility of the whole redox process. In literature, 3-hexylthiophene bearing donor-acceptor type molecules have relatively high polymer oxidation potentials than other common donor units. [76]

In our case, we exploited this property via using PHTBT as the electron donor unit. Since high polymer oxidation potentials and an appropriate band gap result in convenient HOMO-LUMO energy levels, PHTBT can be a strong candidate for p-type photovoltaics. Oxidation-reduction onset values were determined from cyclic voltammetry. Thus, HOMO-LUMO values for the polymer were estimated from electrochemical data (Table 3). From CV experiments, the HOMO and LUMO levels of PHTBT were estimated as -5.5 and -3.0 eV, respectively.

The electrochemical band gap (Eg^{ec}) of PHTBT is higher than the optical gap (Eg^{op}). A similar difference is often observed in conjugated polymers and is usually attributed to the creation of free ions in the electrochemical experiment rather than a neutral excited state. [77] Figure 3.19 presents the both p- and n-type doping properties of PHTBT with definite reversible redox couples at 0.9 V and 0.6 V for p-type doping and -1.97 V and -1.8 V for n-type doping. Consecutive scans also revealed that the PHTBT can be reversibly oxidized and reduced.
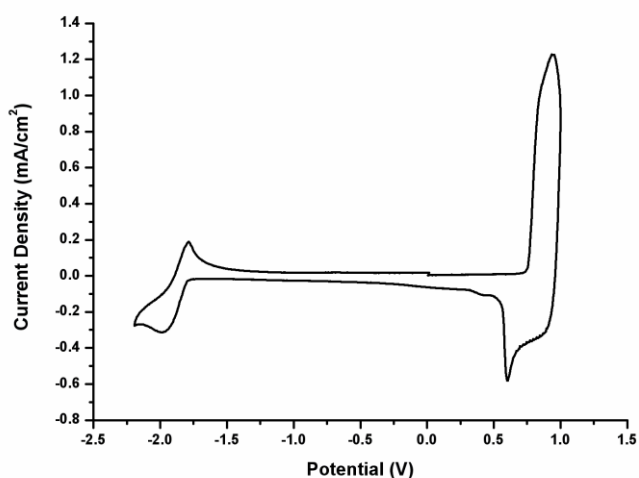
Figure 3. 19 Cyclic voltammogram of PHTBT for both p and n type doping in the presence of 0.1 M ACN/TBAPF$_6$.

Table 3 Cyclic Voltammetry and EVS results of PHTBT (CV was recorded in 0.1 M ACN/ TBPF$_6$ at 100 mV/s scan rate)

HTBT	Oxidation potential (V)		Reduction Potential (V)		Bandgap (eV)		Energy Level (eV) From CV	
	E_{ox}	$E_{onset,ox}$	E_{red}	$E_{onset,red}$	Eg^{ec}	Eg^{op}	HOMO	LUMO
	0.9	0.75	-1.97	-1.8	2.55	1.8	-5.50	-3.0

Anodic and cathodic peak currents revealed a linear relationship as a function of scan rate for both p and n-doping, which indicate that the electrochemical processes are not diffusion limited and are reversible even at high scan rates (Figure 3.20).
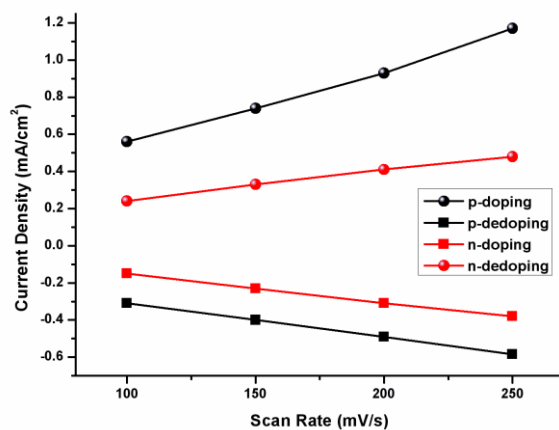
Figure 3. 20 Linear relationships between scan rate and current density of PHTBT film for both p-and n-doping.

3.3.2 Spectroelectrochemistry

The behavior of PHTBT upon doping and dedoping was investigated by UV-vis spectroscopy in a monomer free solution containing ACN with 0.1 M TBAPF$_6$. The undoped PHTBT film displays an absorption maximum in the visible region at 450 nm which indicates an optical band gap of 1.8 eV (calculated from the onset of the π-π* transition for the neutral form). PHTBT is more red shifted than its thiophene based counterpart and result in a higher band gap.[50] This can be due to the long alkyl side chains which can induce steric hindrance with adjacent aromatic rings, leading to destroyed chain coplanarity and increased band gap (≥ 1.8 eV) in thiophene containing donor-acceptor materials. [78]

However; PHTBT can be still considered as a low band gap material for organic photovoltaics. During spectroelectrochemistry, as potential is gradually increased, the peak intensity at 450 nm decreased and new bands at 725 nm and 1310 nm evolved due to the formation of charge carriers such as polarons and bipolarons, respectively (Figure 3.21). Upon doping, no charge carriers were formed until 0.75 V. Then a steep increase in the polaronic region was observed which can be interpreted as the oxidation of the polymer film. As seen in CV (Figure 3.18), no current increase was seen up to 0.75 V which is in accordance with spectroelectrochemical data. A sudden rise in absorbance of polaronic states was recorded at the oxidation potential of the film. [15]
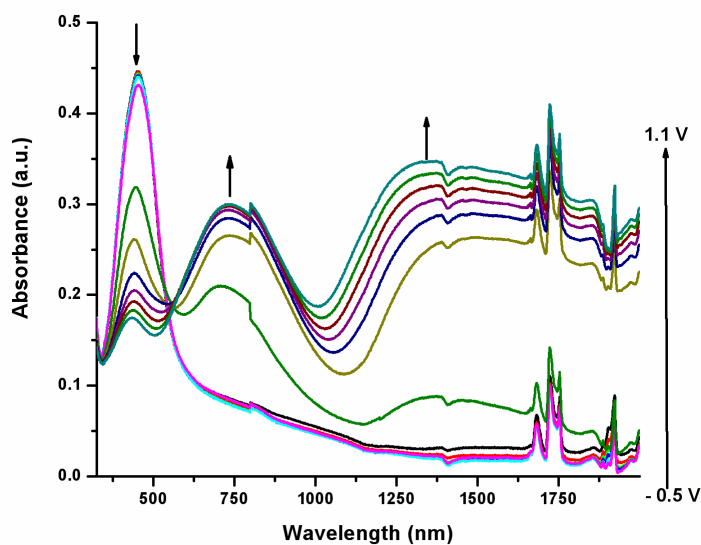
Figure 3. 21 p-Doping electronic absorption spectra of PHTBT between -0.5 V and 1.1 V with 0.05 V potential intervals.

Indications for n-type doping are proved by a reversible redox couple at negative potentials. Additionally and more significantly, a drastic absorption change in the NIR region upon reduction confirms that the polymer is n-dopable. Upon reduction, new bands at around 600 nm and 1250 nm were formed. The difference in the absorption maxima obtained during oxidation and reduction of the polymer indicate the formation of polaron and bipolaron.

When polymer was reduced, a bluish-green (Y: 40.2 x: 0.25 y: 0.29) color was observed and the increase in the absorbance of nearly 35 % in the near-IR region clearly confirmed the formation of charge carriers on the polymer backbone revealing that PHTBT is n-dopable (Figure 3.22).

70
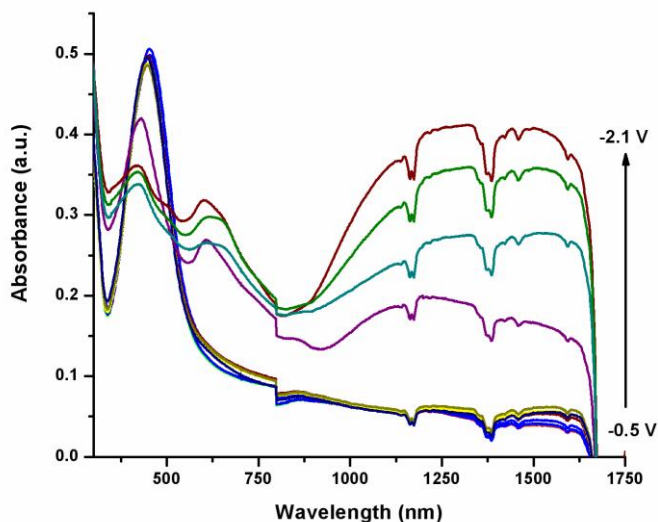
Figure 3. 22 Electronic absorption spectra of PHTBT for n-doping between -0.5 V and -2.1 V with 0.2 V potential intervals.

3.3.3 Kinetic Studies

Transmittance changes and the switching abilities of the polymer film were determined while sweeping the potentials between oxidized and reduced states. PHTBT revealed 35 % transmittance in the visible region at 450 nm. In the near-IR region the optical contrast for the polymer film was found to be 56 % which is considerably sufficient for near-IR applications (Figure 3.23). The long term switching ability was measured, which is an important parameter for device applications. The polymer film was swept between its oxidized and reduced states via chronoamperometry under the same conditions as in-situ UV-vis-NIR spectroscopy. Upon switching, there was less than 10 % charge loss even after 1000 full switches.

71
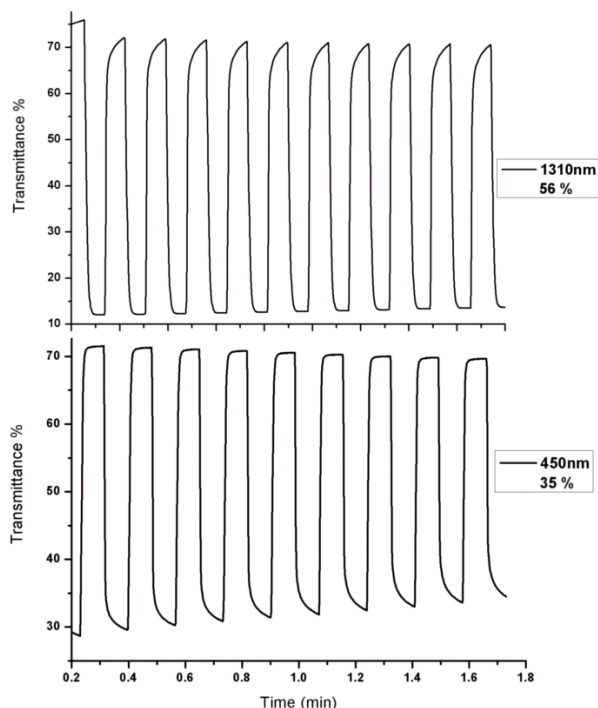
Figure 3. 23 Optical transmittance changes of PHTBT monitored at 450 nm and 1310 nm while switching the potentials between its oxidized and reduced states.

3.3.4 BHJ Solar Cell Fabrication and Characterization

PHTBT was designed to act as an electron donor in BHJ photovoltaic devices with PCBM as the acceptor. Alkyl chains on the polymer backbone improve the solubility of the polymer in common organic solvents such as chloroform, chlorobenzene and THF. Figure 3.24 shows the normalized film absorbances of active layers with different PCBM loadings. As the polymer ratio in PHTBT: PCBM mixture decreases (from 1:1 to 1:4), the characteristic peak of PHTBT was decreased due to the increase of PCBM amount in the mixture. [84]
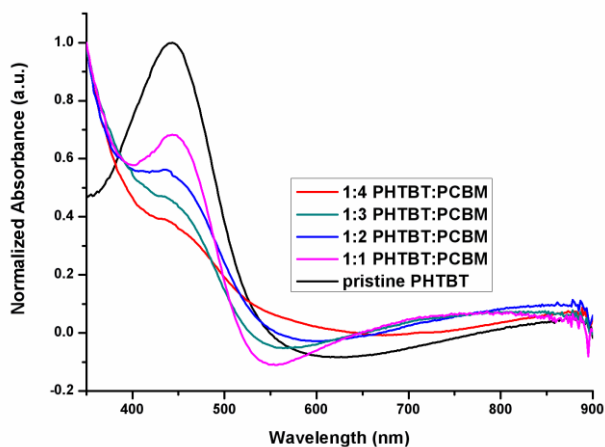
Figure 3. 24 Normalized film absorbance of pristine polymer and mixtures with different PCBM loadings.

The CV-estimated energy levels of PHTBT were used to construct the energy diagram depicted in Figure 3.25.
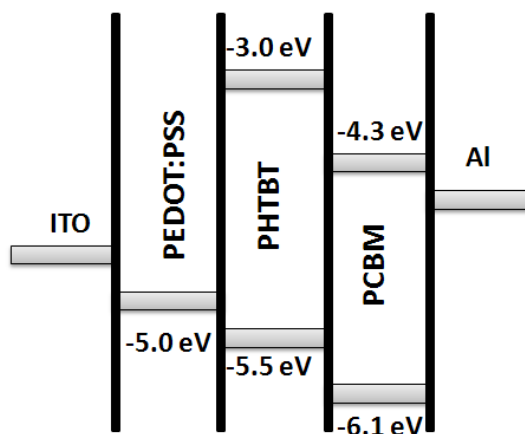
Figure 3. 25 Estimated HOMO-LUMO energy levels for PHTBT and PCBM.

High open circuit voltage obtained for PHTBT can be assigned to the relatively low lying HOMO compared to P3HT. [85] BHJ photovoltaic cells with ITO / PEDOT: PSS / PHTBT:PCBM / Al (100 nm) configuration [ITO, indium tin oxide; PEDOT, poly(3,4-ethylenedioxythiophene); PSS, poly(styrenesulfonate)] were fabricated and characterized. Charge transfer was confirmed by a quenched PL emission by a factor of 20 when adding 50 wt % PCBM (Figure 3.26). Such efficient photoluminescence quenching is the proof of ultrafast photoinduced charge transfer from the polymer to PCBM. [81] Based on these characterizations; the polymer was expected as an interesting candidate to fabricate photovoltaic devices. Various blends of PHTBT: PCBM with different PCBM content were prepared (1:1, 1:2, 1:3, 1:4 w/w; 5 mg:10 mg for 1:2) from chlorobenzene solution.
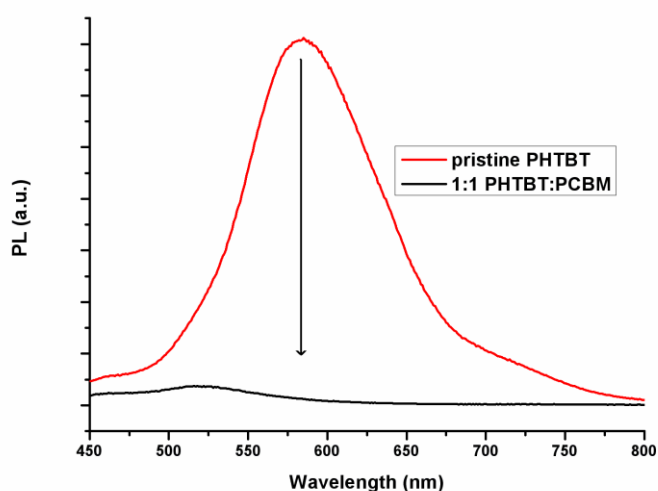
Figure 3. 26 PL quenching of PHTBT upon mixing with PCBM.

After obtaining the spectral response of the active layers and confirming the charge transfer, the photo induced charge generation was determined. Incident

photon to current efficiency (IPCE) is used to get information on the number of photons that contributes to charge generation in a solar cell. Spectral resolved photocurrent measurements showed that the blends generate photo-induced charges nearly over the same range as photons are absorbed in the pristine polymer. [86] In Figure 3.27, the IPCE spectrum spans from 350 to 900 nm and has a maximum at 450 nm with a peak value of 30 % when mixed with PCBM in a ratio of 1:3.
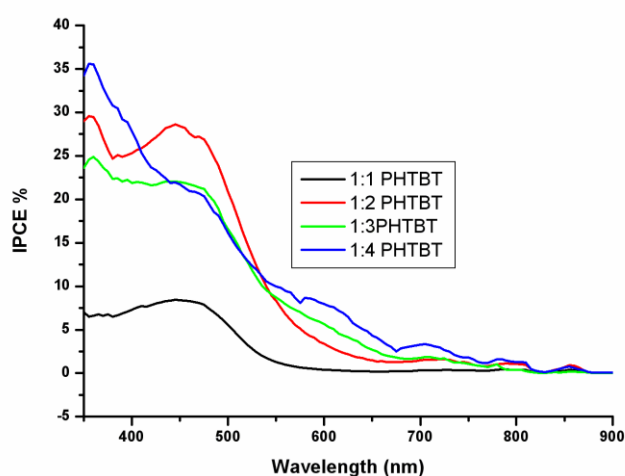
Figure 3. 27 Photocurrent spectra IPCE of photovoltaic devices with PHTBT: PCBM (different ratios) as active layer.

Figure 3.28 indicates the photovoltaic performance of a series of devices fabricated with different PCBM loadings. The short-circuit current (J_{sc}) increases with increasing PCBM content in the devices and reaches a maximum value of 2.35 mA/cm^2 when the blend ratio is 1:3.
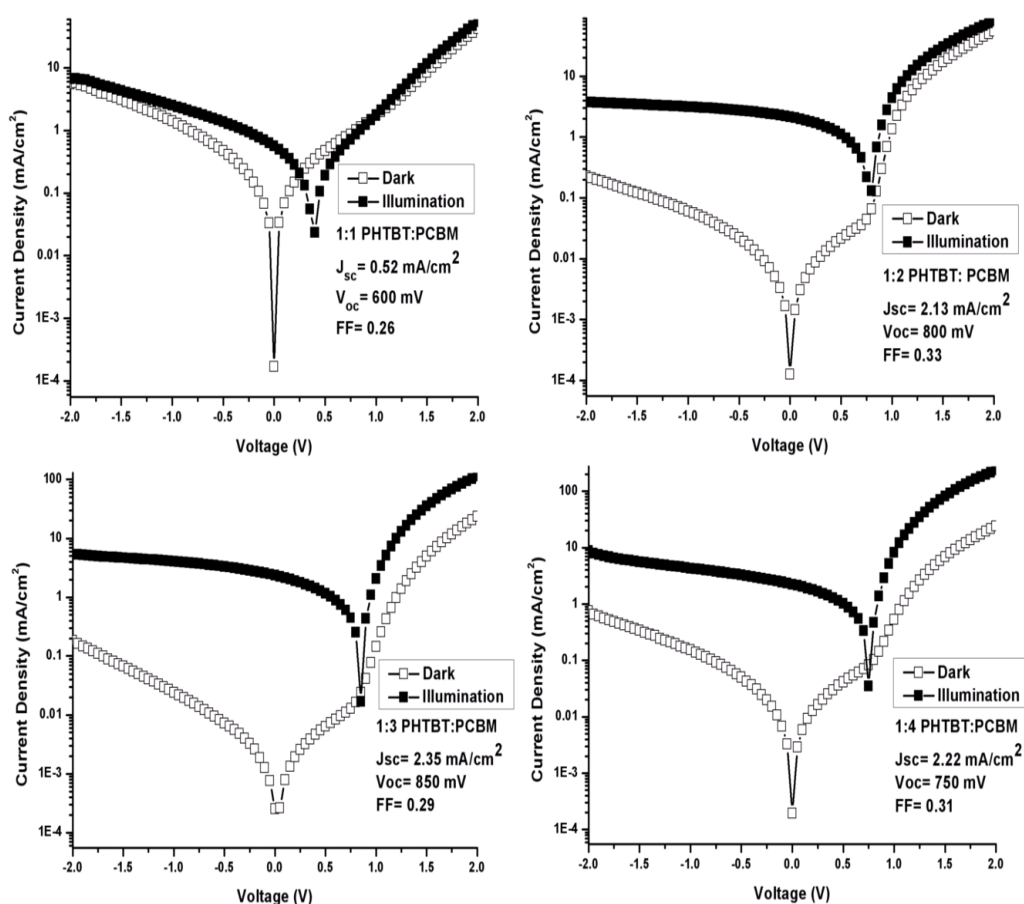
Figure 3. 28 Performance parameters of the measured devices, namely J_{sc} (short-circuit current), V_{oc} (open cicuit voltage) and FF (fill factor) with various PCBM contents under dark and white light illumination (100 mW/ cm^2).

J_{sc} increases from 0.52 mA/ cm^2 (for the device containing 50 wt % PCBM) to 2.13 and 2.35 mA/cm^2 for those containing 66 % and 75 wt % PCBM. However, Jsc decreases for a higher PCBM content (80 %) as shown in Figure 3.28 which means that excess PCBM leads to an imbalanced donor to acceptor ratio. [86] Table 4 summarizes the results obtained from photovoltaic devices

with different ratios of PHTBT:PCBM. [87] The lower J_{sc} values compared to P3HT: PCBM devices may stem from a fast recombination of the separated charges, which is a common problem in polymer: fullerene solar cells. [56] However, the performance of PHTBT: PCBM devives may be optimized and/or increased by varying the metal contacts, using LiF as intermediate layer to the Al contact, annealing, changing the active layer composition, film thicknesses, solvent or acceptor material type (C_{70} and its derivatives), and by functionalization of the donor material PHTBT (which may change the absorption of the active layer and lead to a higher harvesting of photons).

Table 4 Photovoltaic responses obtained from solar cells containing 1:1, 1:2, 1:3 and 1:4 PHTBT: PCBM ratio as active layer.

Active layer ratios (PHTBT:PCBM)	Open Circuit Voltage V_{oc} (V)	Short Circuit Current J_{sc} (mA/ cm^2)	Fill Factor FF
1:1	0.6	0.52	0.26
1:2	0.8	2.13	0.33
1:3	0.85	2.35	0.29
1:4	0.75	2.22	0.31

77

CHAPTER 4

CONCLUSION

The D-A-D type monomers; PyBT and HTBT were synthesized via alkylation, bromination, stannylation and the Stille coupling. Characterizations of the materials were performed by NMR analysis. The polymers of the both monomers were synthesized by electrochemical and chemical methods. Cyclic voltammetry experiments, spectroelectrochemistry, kinetic studies and long-term switching experiments for the polymers were performed in order to investigate the electrochemical and electrochromic properties of the polymers in addition to their photovoltaic characterizations such as PL, I-V and IPCE.

PPyBT was shown that the presence of benzotriazole unit in the polymer backbone led the polymer n-type dopable which is not present in the literature among D-A-D type polymers.The optical contrast of the polymer was 30 % in the visible region and 46 % in the NIR region. As other D-A-D type polymers containing pyrrole as the donor unit, PPyBT also showed the same colors compared to its EDOT based counterpart. This property was attributed to acceptor capacity of benzotriazole moiety. The polymer showed blue color in its neutral state and transmissive blue in the oxidized state. The stability of polymer was remarkable as the charge loss was less than 10 % upon 1000 switches. The polymer was used in solar cells. The low efficiencies and the current were attributed to the poor film formation.However; further study is needed in order to understand the charge transport. Although, the preliminary results showed low values, PPyBT is still significant since DAD type polymers are of high interest in

the field of photovoltaics. The ease of synthesis with relatively high yields makes this polymer the paramount choice in ECD and photovoltaic applications.

Studies for PHTBT showed that both electrochemical and chemical polymers revealed the identical properties in a single material as a very promising multifunctional electrochromic polymer. The polymer has shown to be both p- and n-dopable. The spectroelectrochemistry of the n-doped state was studied at ambient conditions, which signifies it as one of the most stable n-doped polymers in the literature. The polymer revealed very good optical contrast and switching times compared to the homopolymer of the donor unit (polythiophene). PHTBT also revealed 56 % optical contrast in the NIR region which makes it a significant candidate for NIR electrochromic device applications. Strong absorption in the visible region makes this polymer a promising candidate for solar cell applications. Therefore, the BHJ solar cell devices were constructed for PHTBT with PCBM as the acceptor. The results showed that PHTBT can generate photo-induced charges over a range of 350 to 900 nm with a peak value of 30 %.

REFERENCES

[1] H. Shirakawa, E. J. Louis, A. G. MacDiarmid, C. K. Chiang, A. J. Heeger, J. Chem. Soc. Chem. Comm., 1977, 578

[2] C. K. Chiang, Jr. C. R. Fincher, Y. W. Park, A. J. Heeger, H. Shirakawa, E. J. Louis, S. C. Gau, A. G. MacDiarmid, Phys. Rev. Lett., 1977, 39, 1098

[3] C. K. Chiang, M. A. Druy, S. C. Gau, A. J. Heeger, E. J. Louis, A. G. MacDiarmid,Y. W. Park, H. Shirakawa, J. Am. Chem. Soc., 1978, 100, 1013

[4] A. J. Heeger, J. Phys. Chem. B., 2001, 105, 8475

[5] D. Meissner, Photon2., 1999, 34

[6] C. J. Brabec, F. Padinger, N. S. Sariciftci, J. C. Hummelen, J. Appl. Phys., 1999, 85, 6866

[7] M. Granström, K. Petritsch, A. C. Arias, A. Lux, M. R. Andersson, R. H. Friend, Nature, 1998, 395, 257

[8] A. Gandini, M. N. Belgancem, Progress. Polym. Sci. 1997, 22, 1203

[9] A. F. Diaz, K. K. Kanazawa, G. P. Gardini, J. Chem. Soc., Chem. Commun. 1979 635

[10] K. Lee, A. J. Heeger, Synth. Met. 1997, 84, 715

[11] F. Jonas, L. Schrader, Synth. Met., 1991, 41, 831

[12] A. Desbene-Monvernay, P. C. Lacaze, J. E. Dubois, J. Electroanal. Chem., 1981, 129, 229

80

[13] J. H. Burroughes, D. D. C. Bradley, A. R. Brown, R. N. Marks, K. MacKay, R. H. Friend, P. L. Burn, A. B. Holmes, Nature, 1990, 347, 539

[14] G. Grem, G. Leditzky, B. Ullrich, G. Leising, Adv. Mater., 1992, 4, 36

[15] J. Roncali, Chem. Rev., 1997, 97, 173

[16] C. Arbizzani, M. Mastragostini, B. Scrosati, Handbbok of Organic Conductive Molecules and Polymers, Vol. 4, John Wiley & Sons, New York, 1997, 595

[17] W. A. Gazotti, G. Casalbore-Miceli, A. Geri, M.-A. De Paoli, Adv. Mater., 1998, 10, 60

[18] T. F. Otero, Handbook of Organic Conductive Molecules and Polymers, Vol. 4, John Wiley & Sons, New York, 1997, 517

[19] Y. Yang, A. J. Heeger, Nature, 1994, 372, 344

[20] F. Hide, M. Diaz-Garcia, D. Schwartz, M. Andersson, Q. Pie, A. J. Heeger, Science, 1996, 273, 1833

[21] D. O. Reagen, M, Graetzel, Nature, 1991, 353, 737

[22] C. J. Brabec, N. S. Sariciftci, J. C. Hummelen, Adv. Func. Mater., 2001, 11, 15

[23] D. M. De Leeuw, M. M. J. Simenon, A. R. Brown, R. E. F. Einerhand, Synth. Met., 1997, 87, 53

[24] (a) C. J. DuBois, F. Larmat, D. J. Irvin, J. R. Reynolds, Synth. Met., 2001, 119, 321; (b) C. J. DuBois, J. R. Reynolds, Adv. Mater., 2002, 14, 1844: (c) C. J. Dubois, K. A. Abboud, J. R. Reynolds, J. Phys. Chem. B, 2004, 108, 8550

[25] (a) M. J. Rice, Phys. Lett., 1979, A71, 152; (b)W. P. Su, J. R. Schrieffer, A. J. Heeger, Phys. Rev. Lett., 1979, 42, 1698

[26] (a) J. L. Bredas, R. R. Chance, R. Silbey, Phys. Rev. B, 1982, 26, 5843; (b)J. L. Bredas, G. B. Street, Acc. Chem. Res., 1985, 18, 309

[27] G. Zotti, S. Zecchin, G. Schiavon, L. Groenendaal, Chem. Mater. 2000, 12, 2996

[28] A. Kraft, A. C. Grimsdale, A. B. Holmes, Angew. Chem. Intl. Ed., 1998, 37, 402

[29] G. Horowitz, Adv. Mater, 1998, 10, 365

[30] G. Yu, J. Gao, J. C. Hummelen, F. Wudl, A. J. Heeger, Science 1995, 270, 1789

[31] S. A. Sapp, G. A. Sotzing, J. R. Reynolds, Chem. Mater.1998, 10, 2101

[32] E. F. Schubert, J. K. Kim, Science 2005, 308, 1274

[33] C. D. Dimitrakopoulos, P.R.L. Malenfant, Adv. Mater., 2002, 14, 99

[34] C. Reese, M. Roberts, M. Ling, Z. Bao, Mater. Today 2004, 7, 20

[35] (a) D. Wöhrle, D. Meissner, Adv. Mater. 1991, 3, 129; (b) M. Granström, K. Petritsch, A. C. Arias, A. Lux, M. R. Andersson, R. H. Friend, Nature 1998, 395, 257

[36] C. W. Tang, Appl. Phys. Lett., 1986, 48, 183

[37] X. Zhang, T. T. Steckler, R. R. Dasari, S. Ohira, W. J. Potscavage, S. P. Tiwari, S. Coppee, S. Ellinger, S. Barlow, J. L. B. B. Kippelen, J. R. Reynolds and S. R. Marder, J. Mater. Chem., 2010, 20, 123

[38] M. Helgesen, R. Søndergaard and F. C. Krebs, J. Mater. Chem., 2010, 20, 36

[39] A. P. Zoombelt, M. Fonrodona, M. M. Wienk, A. B. Sieval, J. C. Hummelen and R. A. J. Janssen, Org. Lett., 2009, 11, 903.

[40] F. Padinger, C. J. Brabec, T. Fromherz, J. C. Hummelen, N. S. Sariciftci, Opto-Electron. Rev. 8 , 2000, 4, 280

[41] A. Pivrikas, P. Stadler, H. Neugebauer, N. S. Sariciftci, Org. Electron., 2008, 9, 775

[42] J. H. Choi, K. Son, T. Kim, K. Kim, K. Ohkuboa, S. Fukuzumi, J. Mater. Chem., 2010, 20, 475

[43] D. Muhlbacher, M. Scharber, M. Morana, Z. Zhu, D. Waller, R. Gaudiana, C. Brabec, Adv. Mater. 2006, 18, 2884

[44] (a) G. Sonmez, H. B. Sonmez, C. K. F. Shen, R. W. Jost, Y. Rubin, F. Wudl, Macromol.2005, 38, 669; (b) W. Lu, A. G. Fadeev, B. Qi, B. R. Mattes, Synth. Met. 2003, 135-136, 139

[45] (a) S. Varis, M. Ak, C. Tanyeli, I. M. Akhmedov, L. Toppare, Europ. Poly. J., 2006, 42, 2352; (b) B. Yigitsoy, S.Varis, C. Tanyeli, I. M. Akhmedov, L.Toppare, Thin Sol. Films, 2007, 515, 3898; (c) S. Tarkuc, E. Sahmetlioglu, C. Tanyeli, I. M. Akhmedov, L. Toppare, Electrochim. Acta, 2006, 51, 5412; (d) E. Sahin, E. Sahmetlioglu, I. M. Akhmedov, C. Tanyeli, L. Toppare, Org. Electron., 2006, 7, 351

[46] T. A. Skotheim, R. L. Elsenbaumer, J. R. Reynolds, M. Dekker, Handbook of Conducting Polymers, Inc. New York, 1998, 277

[47] M. E Goppelsroder, Compt. Rend. 1876, 82, 331

[48] (a) A. F. Diaz, K. K. Kanazawa, G. P. Gardini, Chem. Commun., 1979, 635; (b) A. F. Diaz, J. I. Castillo, J. Chem. Soc. Chem. Commun., 1980, 397

 [49] G. E. Gunbas, A. Durmus, L. Toppare, Adv. Funct. Mater. 2008, 18, 2026

[50] A. Balan, D. Baran, G. Gunbas, A. Durmus, F. Ozyurt, L. Toppare, Chem. Commun. 2009, 6768

[51] (a) T. Okada, T. Ogata, M. Ueda, Macromol., 1996, 29, 7645; (b) N. Toshima, S. Hara, Prog. Polym. Sci., 1995, 20, 155

[52] (a) K. Yoshino, R. Hayashi, R. Sugimoto, Jpn. J. Appl. Phys., 1984, 23, 899; (b) Delabouglise, R. Garreau, M. Lemaire, J. Roncali, New J. Chem., 1988, 12 155

[53] R. H. Baughman, J. L. Bredas, R. R. Chance, R. L. Elsenbaumer, L. W. Shacklette, Chem. Rev., 1982, 82, 209

[54] G. Zotti, Handbook of Organic Conductive Molecules and Polymers, ed. H. S. Nalwa,Wiley, Chichester, 1997, Vol. 2, Ch. 4.

[55] C. Lungenschmied, G. Dennler, H. Neugebauer, N. S. Sariciftci, M. Glatthaar, T. Meyer, A. Meyer, Sol. Energy Mater. Sol. Cells. 2007, 91, 379

[56] S. Günes, H. Neugebauer, N. S. Sariciftci, Chem. Rev. 2007, 107, 1324

[57] P. Schilinsky, C. Waldauf, C. J. Brabec, Appl. Phys. Lett. 2002, 81, 3885

[58] D. Gebeyehu, C. J. Brabec, F. Padinger, T. Fromherz, J. C. Hummelen, D. Badt, H. Schinler, N. S. Sariciftci, Synth. Met., 2001, 118, 1

[59] N.Camaioni, G. Ridolfi, G. M. Casalbore, G. Possamai, M. Maggini, Adv. Mater. 2002, 14, 1735

[60] Y. Zhao, G. X. Yuan, P. Roche, M. Leclerc, Polymer 1995, 36, 2221

[61] F. Padinger, R. Rittberger, N. S. Sariciftci, Adv. Funct. Mater. 2003, 13, 85

[62] H. Frohne, S. E. Shaheen, C. J. Brabec, D. C. Muller, N. S. Sariciftci, K. Meerholz, ChemPhysChem 2002, 3, 795

[63] (a) R. R. Reyes, K. Kim, D. L. Carroll, Appl. Phys. Lett. 2005, 87, 83506, 1; (b) J. Kim, S. Kim, H. Lee, K. Lee, W. Ma, X. Huong, A. J. Heeger, Adv. Mater. 2006, 18, 572

[64] H. Hoppe, N. S. Sariciftci, J. Mater. Chem. 2006, 16, 45

[65] S. H. Park, A. Roy, S. Beaupre´, S. Cho, N. Coates, J. S. Moon, D. Moses, M. Leclerc, K. Lee, A. J. Heeger, Nat. Photon. 2009, 3, 297

[66] G. Li, V. Shrotria, J. Huang, Y. Yao, T. Moriarty, K. Emery, Y. Yang, Nat. Mater. 2005, 4, 864

[67] A. Balan, G. Gunbas, A. Durmus, L. Toopare, Chem. Mater., 2008, 20, 7510

[68] C. A. Thomas, K. Zong, K. A. Abboud, P. J. Steel, J. R. Reynolds, J. Am. Chem. Soc., 2004, 126 , 16440

[69] E. R. Kötz, H. Neff, K. Müller, J. Electroanal. Chem. 1986, 215, 331

[70] A. Berlin, G. Zotti, S. Zecchin, G. Schiavon, B. Vercelli, A. Zanelli, Chem.Mater., 2004,16, 3667

[71]Bre' das, J. L.; Chance, R. R.; Silbey, R. *Phy.s Re*v. *B* **1982**, *26*, 5843.

[72] C. Winder, G. Matt, J. C. Hummelen, R. A. J. Janssen, N. S. Sariciftci, C. J. Brabec, Thin Sol. Films, 2002, 403-404,373

85

[73] (a) A. T. Taskin, A. Balan, B. Epik, E. Yildiz, Y. A. Udum, L. Toppare, Electrochim. Acta, 2009 54, 5449; (b) A. Durmus, G. E. Gunbas, L. Toppare, Chem. Mater., 2007, 19 , 6247; (c) S. Celebi, A. Balan, B. Epik, D. Baran, L. Toppare, Org. Electron., 2009,   10, 631; (d) G. E. Gunbas, A. Durmus, L. Toppare, Adv. Mater., 2008, 20, 691

[74] (a) S. Günes, D. Baran, G. Günbas, F. Özyurt, A. Fuchsbauer, N. S. Sariciftci, L. Toppare, Solar Energy Mater. Sol. Cell., 2008, 92, 1162; (b) M. A. Khan,W. Xu, K. Haq, Y. Bai, F. Wei, X. Y. Jiang, Z. L. Zhang, W. Q. Zhu, J. Phys. D: Appl. Phys.,2007, 40, 6535; (c) J. W. Maa, W. Xua, X. Y. Jianga, Z. L. Zhanga, Synth. Met., 2008, 58, 810

[75] C. L. Gaupp, D. M. Welsh, R. D. Rauh, J. R. Reynolds, Chem. Mater. 2002, 14, 3964

[76] (a) Y. A. Udum, A. Durmus, G. E. Gunbas, L. Toppare, Org. Electron., 2008, 9, 501; (b) A. S. Ribeiro, Jr. W. A. Gazotti, P. F.Filho, De M. A. Paoli, Synth. Met. 2004, 145, 43; (c) S. Tarkuc, Y. A. Udum, L. Toppare, Polymer 2009, 50, 3458

 [77] J. Hou, M. H. Park, S. Zhang, Y. Yao, L. M. Chen, J. H. Li, Y. Yang, Macromol., 2008, 41, 6012

[78] (a) L. Zhang, Q. Zhang, H. Ren, H. Yan, J. Zhang, H. Zhang, J. Gu, Sol. Energy Mater. Sol. Cells. 2008, 92, 581; (b) J. Hou, Z. Tan, Y. Yan, Y. He, C. Yang, Y. Li, J. Am. Chem. Soc. 2006, 128, 4911

[79] J. C. Hummelen, B. W. Knight, F. LePeq, F. Wudl, J. Yao, C. L. Wilkins, J. Org. Chem., 1995, 60, 532

[80] B. C. Thompson, Y. G. Kim, J. R. Reynolds, Macromol., 2005, 38, 5359

[81] N. S. Sariciftci, Current Opinion in Sol. State and Mater. Sci. 1999, 4, 373

[82] L. M. Campos, A. Tontcheva, S. Günes, G. Sonmez, H. Neugebauer, N. S. Sariciftci, F. Wudl, Chem. Mater., 2005, 17, 4031

[83] H. A. M. van Mullekom, J. A. J. M. Venkemans, E. W. Meijer, Chem. Commun., 1996, 2163

[84] S. Cook, H. Ohkita, Y. Kim, J. J. B. Smith, D. D. C. Bradley, J. R. Durrant, Chem Phys. Lett. 2007, 445, 276

[85] (a) B. C. Thompson, J. M. Fre´chet, J. Angew. Chem. Int. Ed. 2008, 47, 58; (b) E. Bundgaard, F. C. Krebs, Sol. Energy Mater. Sol. Cells 2007, 91, 954; (c) R. Kroon, M. Lenes, J. C. Hummelen, P. W. M. Blom, B. Boer, Polym. Rev. 2008, 48, 531

[86] A. C. Mayer, S. R. Scully, B. E. Hardin, M. W. Rowell, M. D. McGehee, Materials Today, 2007, 10, 28

[87] J. H. Huang, K. C. Li, H. Y. Wei, P. Y. Chen, L. Y. Lin, D. Kekuda, H. C. Lin, K. C. Ho, C. W. Chu, Org. Electron. 2009, 10, 1109